ELSEVIER

Contents lists available at ScienceDirect

Construction and Building Materials

journal homepage: www.elsevier.com/locate/conbuildmat





Role of recycled crushed clay bricks as fine aggregates in enhancing the performance of ferrocement-strengthened RC beams

Md Jihad Miah ^{a,*}, Mohammad Shamim Miah ^b, Noor Md.Sadiqul Hasan ^c, Md.Habibur Rahman Sobuz ^d, Ye Li ^e

- a Civil Engineering, School of Architecture, Technology and Engineering, University of Brighton, Lewes Road, Brighton BN2 4GJ, United Kingdom
- b Institute of Engineering Geodesy and Measurement Systems, Graz University of Technology, Graz 8010, Austria
- Department of Civil Engineering, International University of Business Agriculture and Technology, Dhaka 1230, Bangladesh
- d Department of Building Engineering and Construction Management, Khulna University of Engineering & Technology, Khulna 9203, Bangladesh
- ^e Civil Engineering, Maritime & Environmental Engineering, University of Southampton, Burgess Road, Southampton SO16 7QF, United Kingdom

ARTICLE INFO

Keywords: Recycled crushed clay brick Ferrocement Strengthening Flexural properties Mechanical strength Porosity

ABSTRACT

Ferrocement is a highly effective composite material for enhancing damaged-reinforced concrete (RC) structural elements thanks to its excellent fracture resistance, tensile and flexural strength, crack resistance and durability. This material is applied in thin layers of cement mortar reinforced with steel wire mesh. The resulting structures are strong, lightweight, and cost-effective while allowing for incorporating recycled materials, promoting sustainability and environmental friendliness. Inspired by the outstanding performances of this technique, this study investigated 20 RC beams strengthened using ferrocement. Ferrocement mortar was fabricated with five various substitute rates (0-100 %, with 25 % incremental) of natural sand (NS) by recycled crushed clay brick (RCCB) and two water to cement ratios (w/c) of 0.30 and 0.50. Compressive, tensile, and flexural strength, and porosity of the mortar, were also investigated. In addition, a data-based model was developed and validated with experimental results. A significant enhancement in flexural resistance was recorded for the strengthened beam with up to 50 % RCCB than the unstrengthened beam-USB (15 % and 6 % for w/c of 0.30 and 0.50, respectively, higher than USB), which is aligned with the substantially higher mechanical strength and lower porosity of mortar. It was registered that the damaged beams strengthened with 50 % RCCB were able to nearly reach the stiffness of the USBs and deliver higher deflection (81 % and 31 % for a w/c of 0.30 and 0.50, respectively, higher than 100 % USB) with ductile failure induced by multiple flexural and diagonal cracks. The proposed data-based modelling achieved excellent results, accurately predicting the beams' load deflection and the mortar mixes' strengths and porosity.

1. Introduction

The urgent need to strengthen concrete structures and infrastructures generally arises from the deterioration and ageing of habitation structures and the necessity to upgrade design standards and rectify design mistakes [1–4]. Additionally, unexpected events such as earthquakes, fires, or tsunamis can significantly damage the structures, highlighting the importance of ensuring their load-carrying capacity and structural integrity before using them [5–7]. Numerous research studies indicate that various strengthening techniques can significantly enhance structural strength, ductility and durability. These techniques include carbon fibre-reinforced plastic (CFRP) [4,8,9], jacketing [10,11],

carbonation curing [12], the formation of hydroxyapatite [13], the usage of ultra-high-performance concrete (UHPC) [14,15], and ferrocement composites [16–20]. Several research outcomes reveal that ferrocement composite is favoured due to sound strength properties, local material availability, cost-effectiveness, and straightforward construction process, which are very important in developing countries [16–23].

The detailed design and construction processes for ferrocement composites are discussed in the ACI Committee 549 [23,24], making them a practical choice for strengthening and rehabilitating reinforced concrete structures [16–23,25]. This construction technique uses thin layers of cement mortar reinforced with a network of single and multiple

E-mail address: M.J.Miah@brighton.ac.uk (M.J. Miah).

^{*} Corresponding author.

steel wire mesh, allowing for the formation of strong, lightweight, and flexible structures [22,25]. This technique is commonly used in water tanks, boat building, structural elements (e.g., column, beam, slab) and masonry walls due to its durability and resistance to cracking while experiencing mechanical and dynamic load [16–23,26]. The simple and cost-effective method can be moulded into various shapes, making it versatile for different applications.

The author's previous study investigated reinforced concrete (RC) beams approximately 2 m long fabricated with low-strength concrete with a cylinder compressive strength at 28 days of around 12 MPa. These beams were subjected to unsymmetrical flexural loading conditions [22]. The findings indicated that ferrocement-strengthened beams reveal significantly higher ultimate load-carrying capacities and improved ductile behaviour than un-strengthened beams [22]. Additionally, another study demonstrated that ferrocement can enhance the resistance of slabs against earthquakes, enabling them to withstand moderate to high levels of seismic excitations [26]. Abdallah et al. [18] reveal that utilising chemical anchor bolts within engineered cementitious composite ferrocement resulted in substantial advancements in ultimate stages and cracking, with augments of approximately 92–137 % for cracking and 114–164 % for ultimate levels. Joyklad et al. [19] investigated the structural performance of RC one-way slabs that were retrofitted by ferrocement and fiber-reinforced polymer (FRP) jackets. The authors' [19] findings demonstrated that all slabs displayed more flexural cracks with ductile failure. The utilisation of ferrocement jackets improved the height load and maximum deflection by up to 49 % and 109%, respectively, and the dissipated energy increased by 174% [19]. Joyklad et al. [19] stated that wire mesh type and size greatly affect the performance, where medium and small sized meshes augment ductility, whereas large meshes tend to debond earlier. Further, a parallel orientation to the slab's longitudinal axis suggests more satisfactory performance [19].

The ferrocement construction technique uses thin layers of cementbased mortar where natural sand contributes as filler material, the properties of which dramatically impact the performance of the mortar and strengthened structural members. On the contrary, concrete is produced by mixing cement, coarse aggregate (e.g., stone chips) and fine aggregate (e.g., sand), water and admixtures (if needed). Generally, approximately 20-30 % of the fine aggregate of the concrete volume is used to produce concrete, depending on the grade of the concrete mix [27,28]. Sand is sourced from various locations, including rivers, deserts, coastal areas, and quarries. Natural sand is usually extracted from riverbeds and is commonly used to produce mortar and concrete [28]. Aggregates play a crucial role in reducing the cost of concrete or mortar by filling volume and providing stability, which helps limit shrinkage and enhances mechanical strength and durability [28-30]. Therefore, ensuring high-quality aggregates' availability is essential for cement-based materials' effectiveness. The demand for sand used in concrete production is dramatically increasing due to rapid urbanisation and the growing need for structures and infrastructure. However, some South Asian countries face limited natural sand sources because of their geological features and restricted land available for quarries [29]. Additionally, dredging riverbeds for sand can harm the ecosystem, leading to soil erosion, riverbank damage, and other geological disasters [28-30]. Therefore, finding alternative materials that can replace sand partially and fully in concrete production is crucial. This would help reduce dependence on natural resources and foster the conservation of the environment.

In Asia, many countries use burnt clay brick as a coarse aggregate due to the unavailability of natural sources, which produces a notably higher portion of fine waste product due to more inferior strengths and Young's modulus when crushing bricks to make coarse aggregate. These enormous fine waste materials are not generally used as building construction materials and are dumped into landfills. The author's previous study revealed that this waste clay brick fine product has a rough surface texture that provides robust bonding with the cement and boosts the

strength properties, durability and shrinkage behaviour [29]. The compressive, tensile, and flexural strength were improved by 25 %, 31 % and 31 %, respectively, for mixing with 50 % waste clay brick and 50 % sand compared to the control mortar specimens made with 100 % sand [29]. Huang et al. [31] investigated the recycling of crushed waste clay bricks as aggregates in cement mortars. The authors [31] stated that mortar with waste clay bricks exhibited significantly higher mechanical strength (17-71 % for compressive strength and 2-25 % for flexural strength) and lower water absorption than the control mortar cast with natural river sand. The TG-DSC analysis reveals that the hydration degree of cement in the mortar made with waste clay bricks was higher than that of the control mortar with sand. It was also found that the waste clay bricks were tightly bonded by cement paste in the mortar, ensuring a robust interfacial transition zone (ITZ) and higher mechanical strength [31]. Furthermore, the porosity of the mortar decreased with the increased content of waste brick in the mortar up to 50 % replacement; beyond that, the porosity increased [29]. On the contrary, it was found that the shrinkage was increased with the increased content of waste brick aggregates [29]. These outcomes indicated that successfully applying waste clay brick to mortar and concrete production could save landfill space, reduce the demand for natural sand (limiting soil erosion, damage to riverbanks, and other geological catastrophes), and provide environmental benefits without compromising the strength and durability properties of mortar [29,31]. Generally, the collection of natural sand contributes to higher CO2 emissions due to several environmental impacts. The extraction process disrupts ecosystems, reduces the capacity of vegetation to sequester carbon, and leads to land degradation. Additionally, increased erosion and emissions from machinery used in transportation further raise carbon output. In contrast, the above-mentioned better properties of mortar fabricated with waste clay brick as a replacement for sand can significantly lower carbon dioxide emissions by several metric tons each year, thereby supporting sustainable development and environmental protection.

Research on strengthening RC structural elements using ferrocement is relatively limited but growing. The research mentioned above [16–20, 22,25,26] on ferrocement-strengthening masonry buildings, RC beams and RC slabs explored various aspects, such as tensile and flexural load-bearing capacity. These studies highlight the potential benefits of ferrocement, including cost-effectiveness, ease of construction, and durability. However, most of the studies used natural sand (NS) as fine aggregate in ferrocement, whereas utilising waste material as a replacement for natural sand is limited, and the mechanisms are not known in detail in the literature. In addition, finite element models are mainly used to predict the behaviour of structural elements under various loads, ensuring safety, optimising designs for cost-effective solutions, and validating experimental results. They help understand the complex interactions between ferrocement and concrete, which are difficult to evaluate through experiments alone. While numerical modelling is essential for improving strengthened RC beams, no validated data-based model for ferrocement-strengthened RC beams is available in the literature. To the authors' best knowledge, no numerical findings are available for the ferrocement-strengthening with waste clay bricks, especially for a data-based model. This lack of knowledge needs further study to fully establish standardised guidelines and best practices for using ferrocement in structural strengthening, utilising waste materials, and promoting sustainability. Inspired by the success of a previous study [29] due to better-strengthened durability properties, this work aims to utilise recycled crushed clay brick (RCCB) as various replacements for NS to produce the mortar for the ferrocement strengthening technique. The properties and strength mechanism of RCCB ferrocement mortar are not known. To this aim, an extensive experimental program has been designed to study the mechanical properties and porosity of RCCB ferrocement mortar fabricated with two water-cement ratios (w/c) of 0.30 and 0.50 and the flexural performance of ferrocement-strengthened RC beams. The RCCB is produced when coarse aggregate is crushed by several years old waste clay brick and

thus generally dumped after demolishing the building. This differs from the previous study by Miah et al. [29], where burnt clay brick waste was produced from new bricks, and also sand was coarser sand, while fine sand was used in this study. These old waste bricks were collected from old demolished masonry buildings. They used to produce coarse aggregate for another project, which generated RCCB and was considered as a fine aggregate to produce ferrocement mortar. The utilisation of RCCB as fine aggregate is an eco-friendly material and eliminates the dumping crisis from both old bricks and RCCB, reducing the demand for natural sand and reducing significant amounts of CO2 emission from the atmosphere by minimising burning clay. Ultimately, this practice contributes to sustainable development and safeguarding the environment. Additionally, various data-driven models were developed based on experimental results, including mid-span load-deflection profiles and compressive strength, tensile strength, and flexural strength and porosity measurements. The outcomes of these models were systematically compared with experimental outcomes.

2. Experimental methodology

2.1. Materials properties

Crushed well-burnt clay brick was used as coarse aggregate, and sand was used to cast the reinforced concrete (RC) beams, which were fabricated using crushed well-burnt clay brick as coarse aggregate and sand as fine aggregate. Different properties of brick coarse aggregate (BCA) and coarse sand (CS) were tested for specific gravity, absorption capacity, unit weight, and sieve analysis as following ASTM C127 [32], ASTM C128 [33], ASTM C29 [34], ASTM C136 [35], respectively. While the Los Angeles abrasion, flakiness index, elongation index, crushing value, impact value, and angularity number were investigated only on the BA as per ASTM C131 [36] and BS EN 1097–3:1998 [37]. The tested properties of BA and CS are shown in Table 1. CEM II 42.5 N cement as a binder was considered, which consisted of approximately 80–94 % clinker, 6–20 % supplementary cementitious materials (slag and fly ash), and 0–5 % gypsum.

Natural sand (NS) and recycled crushed clay brick (RCCB) were used as fine aggregates to strengthen RC beams using ferrocement mortar. RCCBs were produced enormously when coarse aggregate was produced by crushing several years-old waste clay bricks. Generally, these waste bricks are dumped after demolishing the building. These old waste bricks were collected from several-year-old demolished masonry buildings and utilised to produce coarse aggregate for another project, which generated RCCB enormously and was used as fine aggregate to produce ferrocement mortar. The original images of NS and RCCB are illustrated in Fig. 1a, b. The original and Scanning Electron Microscopy (SEM) images of NS and RCCB (see Fig. 1d, e) showed that RCCB has excellent surface roughness and is more angular as it is produced while crushing the bricks. On the opposite, the particle shape of NS is rounded, less angular, and uncrushed, as it is sourced from a river.

Both NS and RCCB were sieved following the ASTM C136 [35]

Table 1Properties of aggregates (brick coarse aggregate: BA, and Coarse sand: CS) used to cast reinforced concrete beams.

	BCA	CS
Fineness modulus	6.35	2.8
Unit weight	1115kg/m^3	1535kg/m^3
Absorption capacity	22 %	3.2 %
Specific gravity	2.2	2.5
Los Angeles abrasion	40.2 %	-
Flakiness index	13.4 %	-
Elongation index	40 %	-
Crushing value	40.3 %	-
Impact value	27.9 %	-
Angularity number	9.3	-

standard sieve, and the grain size distributions are reported in Table 2. Five substitute levels (0, 25, 50, 75, and 100 %) of NS by RCCB were studied, and therefore, the sieve analysis was also conducted for all replacement levels. It was observed that 4.75 mm was the maximum size for both NS and RCCB, and the percentage of this size was minimal. It was found that RCCB has a greater amount of smaller particles of size 0.15 mm and pan than NS (see Table 2 and Fig. 1b). A higher amount of smaller size particles is expected to fill the microvoids of the mortar matrix, which improves the microstructure (i.e., lowering the porosity and pore connectivity) and results in robust strength and durability properties. The Fineness modulus (FM) of 100 % NS, 25 % RCCB, 50 % RCCB, and 100 % RCCB are 2.33, 2.90, 3.01, 3.15 and 3.04, respectively.

Both NS and RCCB were evaluated for specific gravity, water absorption capacity, and unit weight according to ASTM C128 [33] and ASTM C29 [34]. The unit weight and specific gravity of RCCB (1120 kg/m³ and 1.73) were inferior to the NS (1594 kg/m³ and 2.22), which ensures a more inferior dry density of ferrocement mortar fabricated with RCCB than NS. In contrast, higher absorption capacity was found for RCCB (12.92 %) than NS (5.71 %). However, steel wire mesh was utilised to strengthen the RC beams using ferrocement, and the original and SEM images are shown in Fig. 1c, f. The same binder (CEM II 42.5 N) was considered to make ferrocement mortar that was used to cast RC beams. The binder's consistency, initial and final setting time, compressive strength and tensile strength were carried out as per ASTM C187 [38], ASTM C191 [39], ASTM C109 [40], and ASTM C307 [41], respectively, and the results of the test are displayed in Table 3.

2.2. Preparation of specimens and test setup

2.2.1. Un-strengthen specimens

A total of 22 RC beams with a length of 750 mm, width of 125 mm, and height of 200 mm (Fig. 2) were fabricated to evaluate the flexural performance of un-strengthened and strengthened RC beams. Among 22 beams, 20 beams for strengthening (10 beams for 5 different RCCB content at water to cement ratio-w/c of 0.30 and 10 for another w/c of 0.50; 2 beams for each case), and 2 beams for un-strengthening were used.

All RC beams were constructed with 2 steel bars of diameter 10 mm as tension reinforcement at the bottom face. Meanwhile, in the upper portion (i.e., compression area), 2 steel bars of diameter 8 mm were used, as illustrated in Fig. 2. It is noted that all concrete specimens as virgin condition were cast at a constant w/c of 0.55 and cement amount of 350 kg/m³. The mixture proportions of the concrete mix are shown in Table 4. The slump value as workability of the fresh concrete mix was measured according to ASTM C143 [42], and the fresh concrete temperature was monitored via a digital concrete thermometer; the values were 22.2 mm and 26.9 °C, respectively. To evaluate the mechanical strength and durability of concrete, compressive strength and splitting tensile strength of concrete were tested on the cylindrical specimens with 200 mm in height and 100 mm in diameter following ASTM C39 [43] and ASTM 496 [44], respectively and tested at 28 days. In contrast, the porosity of the concrete was investigated following NF P18-459 [45]. The concrete properties are given in Table 4.

All beams were tested after 28 days of water curing and subjected to four-point incremental static loads on the simply supported until nearly/complete failure of the beams. As mentioned earlier, two RC beams (unstrengthened) were tested until they collapsed and considered a reference case. During the flexural tests, the deflection behaviour of the beams was monitored using 3 Linear Variable Displacement Transducers (LVDTs) placed at the midpoint and 200 mm to the left and right side, as shown in Fig. 2. The mid-span load-deflection curves of two unstrengthen beam (USB) is illustrated in Fig. 3, and the failure load of the two beams was 180.9 kN and 186.5 kN (average collapse load: 184 kN), while the major flexural and diagonal cracks were around 150 kN.

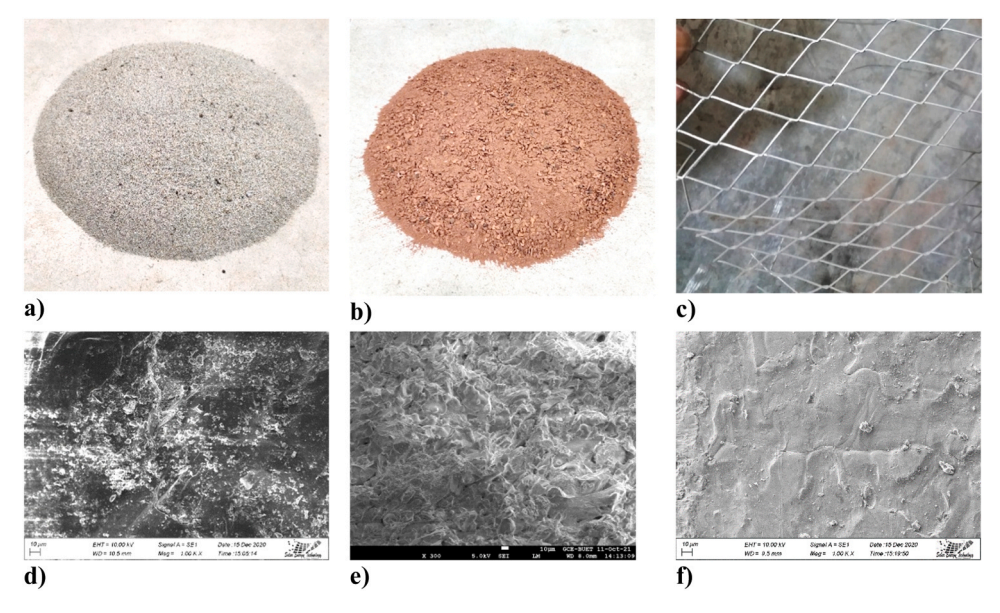


Fig. 1. Image of NS (a), RCCB (b), steel wire mesh (c), and SEM images of NS (d), RCCB (e), and steel wire mesh (f).

Table 2Grain size distribution of NS and different percentages of RCCB.

Sieve Opening	Percentage passing				
[mm]	100 % NS	25 % RCCB	50 % RCCB	75 % RCCB	100 % RCCB
9.5	100	100	100	100	100.00
4.75	100	99.20	98.65	97.55	93.31
2.36	100	86.62	81.20	80.42	74.52
1.19	91.40	67.00	60.61	57.86	50.52
0.59	55.68	33.07	35.95	29.12	32.41
0.3	15.96	17.36	13.50	11.33	25.75
0.15	4.20	7.10	8.86	9.08	19.28
Pan (g)	21	35.5	44.32	45.42	96.4
FM	2.33	2.90	3.01	3.15	3.04

Table 3 Physical properties of the binder.

Properties	Observed Values
Normal consistency [%]	28.20
Initial setting time [min]	98
Final setting time [min]	356
Compressive strength [MPa] at 3-day, 7-day, 14 and	13.90, 19.96, 24.70 and
28-day	30.74
Tensile strength [MPa] at 3-day, 7-day, 14 and 28-day	1.35, 1.88, 2.19 and 2.88

2.2.2. Strengthened specimens

All the RC beams were loaded until 150 kN as the major flexural and diagonal cracks were noticed in two of the un-strengthen beams (Fig. 4a). Subsequently, the beams were unloaded, and the beam surfaces were roughened using metallic hammers. The roughening (i.e., chipping) of the beam surfaces was done very carefully to avoid further damage to the beams. Afterwards, the beam surfaces were cleaned using an iron brush to remove all the concrete dust and debris. A single layer of steel wire mesh was wrapped on three surfaces of the beam (i.e., U-shape jacketing) and fixed with stainless steel nails and screws (Fig. 4b). Later, the cement-based mortar ware applied on the beam surfaces, as shown in Fig. 4c. The average thickness of the ferrocement mortar was about 15 mm, which maintained the original dimensions of the beams carefully.

The cement mortar was poured carefully across the wire mesh to prevent air voids from forming between the parent concrete surfaces, the wire mesh, and the cement mortar, ensuring a better bond and greater strength. To study the role of RCCB on the flexural performance of RC-strengthened beams, five replacement substituents (0, 25, 50, 75, and 100 %) of NS by RCCB were studied. The weight basis mix design with two w/c of 0.30 and 0.50 was used. Superplasticiser as a chemical admixture (0.5 % weight of cement) was used for the mixes with only w/c of 0.30 to improve fresh mortar workability. As reported earlier, the water absorption capacity of RCCB is about 2.2 times higher than the NS (water absorption is 12.9 % for RCCB and 5.7 % for NS); therefore, the sand-to-cement ratio was fixed the same at 2.5 % for both w/c of 0.30 and 0.5. The idea was to introduce more water to the mortar mix to see the effect on the properties. The mix design of the mortar mixes is summarised in Table 5.

As discussed in Section 2.2.1, in a similar way, all RC-strengthened beams were tested after 28 days of water curing and subjected to four-point incremental static loads until collapse. The deflection of the RC beams was registered with 3 LVDTs, as shown in Fig. 2. After the failure of the beams, the crack patterns and their positions were measured. To deeper understand the role of RCCB on the performance of ferrocement mortar, the mortar specimens tested for compression, tension, and flexural strength as per ASTM C143 [42], ASTM C109 [40], ASTM C307 [41], and ASTM C348 [46], accordingly, on the same day of RC beam tests (i.e., 28 days). The dry density of mortar cubes (50 mm) was also registered before the compression test on the same samples. To further understand the durability of mortar, the total porosity of the mortar mixes was conducted following NF P18-459 [45].

2.3. Data-based modeling

Data-based modelling is gaining attention due to its versatility and applicability in various areas of science and engineering. It would be great to have from experiments because that is the closest true representation of the real-world problem. However, performing tests may not always be possible due to many underlying drawbacks such as cost, time, and manpower. Hence, it might be useful to have a model that can be utilised as an alternative to doing tests to get an idea of the expected results, e.g., loads, deflections, strain, or strength. Different models have been developed within this context based on the experimental outcomes. More precisely, the models have been developed for (i) the load-deflection profiles of the beams, (ii) the strengths (e.g., compressive, tensile and flexural), and (iii) porosity. Later, the performances of the models were evaluated and compared with the counterpart, e.g.,

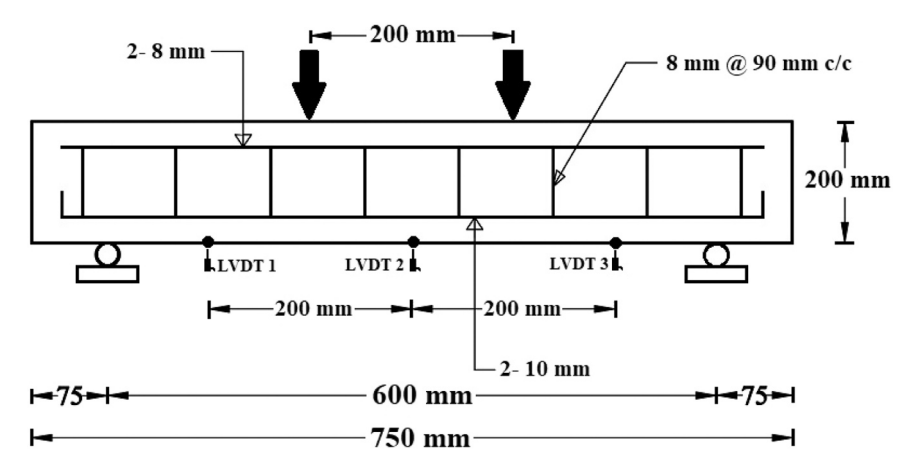


Fig. 2. Reinforcement detailing of the beam and four-point flexural test setup.

Table 4
Mix design and concrete properties.

Mix design [kg/m ³]		
Cement	350	
Brick coarse aggregate (BCA)	772	
Natural sand (NS)	829	
Water	193	
Properties		
Slump [mm]	22.2	
Temperature of fresh concrete [°C]	26.9	
28-day compressive strength [MPa]	22.24	
28-day splitting tensile strength [MPa]	2.12	
28-day modulus of elasticity [GPa]	17.7	
28-day porosity [%]	30.22	

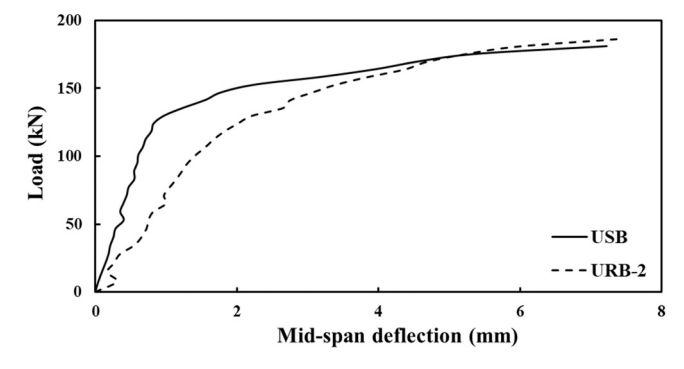


Fig. 3. The load-deflection registered at mid-span of two un-strengthen beams (USB).

experimental data. It is observed that all developed models are capable of rendering the true data quite efficiently. Further, all the models were validated using a different data set. It needs to be mentioned that a sample model for each case (e.g., load-deflection, strength, porosity) has been presented only. This is because all the models would look alike more or less, but their coefficients are not the same. The polynomial regression models are studied due to their simplicity and robust performances [47,48]. The aforementioned models perform a least-squared method that reduces the variance of the unbiased estimator of the desired coefficients (as shown in Tables 6, 7 and 8). It needs to be mentioned that the model's coefficients are not constant for all cases. In other words, models parameters need to be updated whenever a different design parameter is induced, such as design mix ratio. The main input/independent variables for all models are shown on the x-axis, e.g. displacements, % of RCCB. As a side note, the data-based models were developed using MATLAB® R2020a. A sample model for

maximum deflection at the mid-span of the RC beam can be described in Eq. 1. Alternatively, the aforementioned equation can be written as depicted in Eq. 1a with a set of coefficients and variables.

$$\Delta_{c} = \begin{bmatrix} \beta_{1} & \beta_{2} & \beta_{3} & \beta_{4} \end{bmatrix} \begin{Bmatrix} 1 \\ x \\ x^{2} \\ x^{3} \end{Bmatrix}$$
 (1)

$$\Delta_c = -2.7897 + 97.5959x - 17.86669x^2 + 1.0784x^3 \tag{1a}$$

where, β_1 , β_2 , β_3 , β_4 are coefficients, x is the main independent variable, and Δ_c is the output at the mid-span of the beam.

Similarly, a sample model for strengths data can be described in Eq. 2. Further, this equation can be expressed as shown in Eq. 2a.

$$\sigma = \begin{bmatrix} \alpha_1 & \alpha_2 & \alpha_3 & \alpha_4 \end{bmatrix} \begin{Bmatrix} 1 \\ r \\ r^2 \\ r^3 \end{Bmatrix}$$
 (2)

$$\sigma = 29.3871 + 0.2862r - 0.0052r^2 + 0.0001r^3 \tag{2a}$$

where α_1 , α_2 , α_3 , α_4 are coefficients, r is the main independent variable, e.g., RCCB ratio, σ is the output.

Lastly, a sample model for porosity data is given in Eq. 3. Similarly, an additional Eq. 3a is provided herein for a better understanding of Eq. 3.

$$\emptyset = \begin{bmatrix} \partial_1 & \partial_2 & \partial_3 & \partial_4 \end{bmatrix} \begin{Bmatrix} 1 \\ r \\ r^2 \\ r^3 \end{Bmatrix}$$
(3)

$$\emptyset = 26.8948 - 0.0239r - 0.0025r^2 + 0.0002r^3$$
 (3a)

where ∂_1 , ∂_2 , ∂_3 , ∂_4 are coefficients, r is the main independent variable, e. g., RCCB ratio, \emptyset is the output.

3. Experimental results and discussion

3.1. Load-deflection behaviour of RC beams

The mid-point load-deflection curves of two un-strengthen beams (USB) and 20 strengthened RC beams using ferrocement mortar fabricated with various replacement levels of NS by RCCB with two different



Fig. 4. Strengthening of beams utilising the ferrocement method: (a) damaged the beam nearly collapsed, (b) roughening the strengthened surface of the beams and wrapped with steel wire mesh U-shape jacketing, and (c) application of cement-based mortar on the beam surfaces.

Table 5Mix design of mortar mixes [kg/m³].

	Mix ID	Cement	Fine Aggregates		Water
			NS	RCCB	
w/c = 0.30	100 % NS	557	1393	0	167
	25 % RCCB	557	1045	269	167
	50 % RCCB	557	696	538	167
	75 % RCCB	557	348	807	167
	100 % RCCB	557	0	1076	167
w/c = 0.50	100 % NS	500	1251	0	250
	25 % RCCB	500	938	242	250
	50 % RCCB	500	625	483	250
	75 % RCCB	500	313	725	250
	100 % RCCB	500	0	966	250

Table 6Coefficients of a sample model for load-deflection relationship.

Coefficients	Coefficients Values	95 % confidence bounds
β_1	-5.429	(-10.79, -0.07104)
β_2	92.4	(84.78, 100)
β_3	-16.71	(-19.34, -14.07)
β_4	1.051	(0.8046, 1.297)

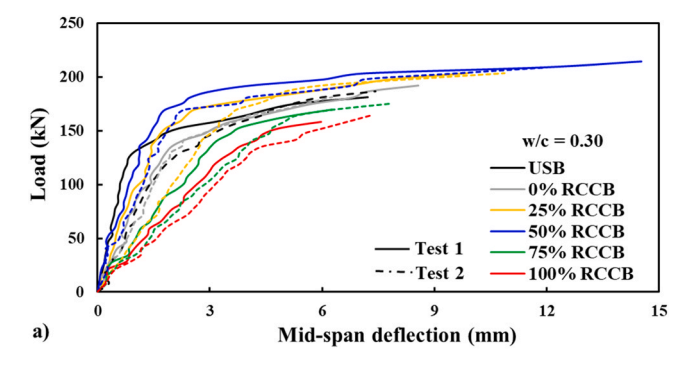
Table 7Coefficients of a sample model for the compressive strength.

Coefficients	Coefficients Values	95 % confidence bounds
α_1	36.84	(31.38, 42.3)
α_2	0.4357	(-0.12, 0.9914)
α_3	-0.007604	(-0.02172, 0.006509)
α_4	2.453e-05	(-6.823e-05, 0.0001173)

Table 8Coefficients of a sample model for the porosity.

Coefficients	Coefficients Values	95 % confidence bounds
∂_1	21.23	(18.25, 24.2)
∂_2	-0.05167	(-0.3541, 0.2507)
∂_3	-0.000784	(-0.008464, 0.006896)
∂_4	1.717e-05	(-3.331e-05, 6.765e-05)

w/c are illustrated in Fig. 5. It was found that the strengthened RC beams using ferrocement mortar fabricated with 100 % NS (0 % RCCB) exhibited higher flexural load compared to USB. The failure loads of two strengthened beams using ferrocement with 100 % NS mortar are 180.9 kN and 192.1 kN for w/c of 0.30, respectively. In contrast, the two USBs failure loads are 180.9 kN and 186.5 kN (average collapse load: 184 kN). Hence, the strengthened beams reached the virgin USBs failure loads and enhanced by about 2 % higher than USB. The present study employs single-layer ferrocement made from thin steel wire mesh, which offers excellent tensile strength and better confinement for damaged RC beams [16-20,22,26]. As there are no coarse aggregates, the thin sections of the ferrocement allow for a higher reinforcement ratio—meaning more mesh layers per unit thickness. This enhancement in strength occurs without adding excessive weight. The ferrocement steel wire mesh distributes stresses more evenly, preventing localised cracking and improving the load-carrying capacity of the strengthened RC beams [22,26]. Furthermore, the ferrocement mortar, composed of a rich cement mixture, also constructs a dense microstructure that forms a strong bond with the steel wire mesh and the parent concrete (roughening old concrete surfaces by chipping). This bond facilitates efficient stress transfer from the brittle mortar to the more ductile steel wire mesh, resulting in increased resistance to cracking [22,26]. Consequently, the beams can support greater loads without significant deflection or the risk of failure in the strengthened RC beams.



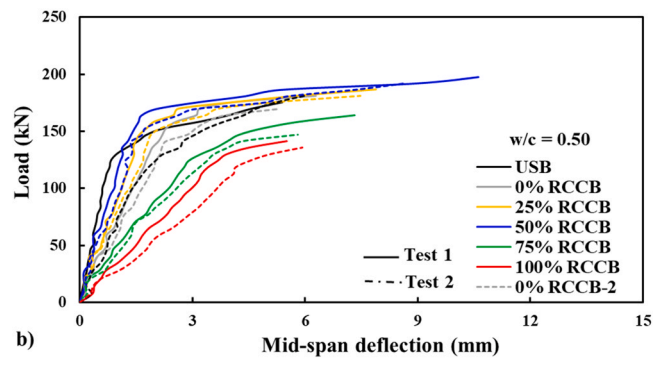


Fig. 5. Load versus mid-span deflection profiles of RC beams strengthened using ferrocement mortar with different percentages of RCCB with w/c of 0.30 (a) and 0.50 (b).

An important observation is that incorporating RCCB in the ferrocement mortar augments the flexural load-carrying capability of strengthened RC beams. An increase in flexural load is observed, up to 50 %, in the replacement of NS by RCCB, while an enhancement in the RCCB amount above the 50 % substituent level leads to a decline in the flexural load of beams (Fig. 5). For example, the mean failure load of two strengthened RC beams using ferrocement mortar with 0 %, 25 %, and 50 % RCCB are 187 kN, 203 kN and 212 kN, which are augmented by 2 %, 11 % and 15 %, respectively, for w/c of 0.30 than to the USB. In contrast, the average failure load of strengthened RC beams at w/c of 0.50 are 175 kN, 184 kN and 195 kN for 0 %, 25 %, and 50 % RCCB, respectively, which enhanced by -5 %, 0 %, and 6 %, compared to the USB, as shown in Fig. 6. It should be noted that the damaged beam strengthened using ferrocement with up to 50 % RCCB mortar enhances the stiffness of the beam, which is more evident with the 50 % RCCB mortar. The slope of the load-deflection curves was quite steep initially, and it decreased and later became zero near the failure load. The higher flexural load and recovery of the stiffness of the strengthened RC beams fabricated with RCCB could be due to the stronger bond among the parent concrete, steel wire mesh (provides additional tensile strength

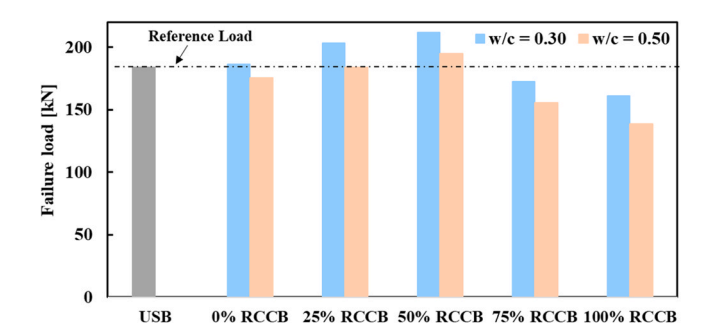


Fig. 6. The failure load of the un-strengthened beam (USB) and beams strengthened using ferrocement mortar with different percentages of RCCB.

and confinement to the beams, which delays and limits the formation of cracks), and RCCB mortar.

This elevated flexural load of the strengthened RC beams is consistent with the strength properties and porosity of the mortar fabricated with RCCB, explained in Section 3.3. It was registered that the mortar fabricated with RCCB has remarkably higher mechanical (compressive, tensile and flexural) strength and lower porosity. The RCCBs have a rough surface texture resulting from the production process, which involves crushing bricks. As shown in Fig. 1, the scanning electron microscopy image of RCCB is higher angular and possesses a rougher surface than the NS. This higher surface roughness enriches the bond between RCCB mortar and the parent concrete (roughening old concrete surfaces by chipping), delays debonding at their interface, and offers a better load-bearing capability of the strengthened beams. Similar behaviour was reported by Miah et al. [29]. The compressive, tensile, and flexural strength were improved by 25 %, 31 % and 31 %, respectively, for mixing with 50 % waste clay brick as replacement of sand compared to the control mortar specimens made with 100 % sand [29]. The increase in mechanical strength can be attributed to the highly angular shape, coarser particle size, and rougher surface texture of waste clay bricks compared to sand. These characteristics facilitate better interlocking between the cement paste and the waste bricks, enhancing mechanical strength [29]. In another study [30], it was reported that slump value dropped dramatically when a crushed waste steel slag powder was used compared to the natural sand. In contrast, compressive, tensile, and flexural strength was increased by 45 %, 72 % and 56 %, respectively, when sand was entirely replaced by crushed slag powder [30]. It was stated that the waste slag powders are highly angular and have a rough surface texture due to the mechanical crushing process, resulting in the fresh mortar's decreased mobility due to better particle interlocking. These properties improved the strength of the interfacial transition zone (ITZ) between the cement paste and rough slag powder, leading to higher strength. In contrast, natural sand was relatively round and uncrushed, which enhances flowability due to its rolling effect and offers relatively weak ITZ between the cement paste and sand, leading to lower mechanical strength [29,30]. Furthermore, Huang et al. [31] reported that the hydration degree of cement in the mortar made with waste clay bricks was higher than that of the control mortar with sand, which enhanced the mechanical performance. The authors [31] also stated that cement paste in the mortar tightly bonded the crushed waste clay bricks, ensuring a robust interfacial transition zone (ITZ) and higher mechanical strength.

Furthermore, Table 2 and Fig. 1b indicate that the RCCB has significantly more finer particles (0.15 mm to pan) than normal sand (NS). This abundance of smaller particles is expected to fill the micro and meso pores in the mortar matrix, reducing porosity (as discussed in Section 3.3.3) and permeability while densifying the interfacial transition zone (ITZ). As a result, this should improve the mechanical strength compared to 100 % normal sand. The considerably higher tensile strength of steel wire mesh and the robust mechanical properties and lower porosity (lower pore network, i.e., lower permeability) of mortar fabricated with RCCB could be the main reason for enhancing the flexural performance of strengthening RC beams compared to the USBs. The visual inspection and in Fig. 1c, f reveal that steel wire mesh has higher surface roughness, which helps to boost the bonding with the RCCB mortar and offers a better load-bearing capability of the strengthened beams.

It is found that the ferrocement mortar fabricated with a low w/c of 0.30 is more effective for improving strength and stiffness than the low w/c of 0.50. The failure load of RC beams strengthened with 100 % NS (0 % RCCB) is 5 % lower for the w/c of 0.50 than the USBs, while it is around 2 % higher for the w/c of 0.30. In contrast, the RC beams strengthened with 25 % and 50 % RCCB recovered and exhibited higher flexural load for both w/c of 0.30 and 0.50, which is about 11 %-15 % and 0 %-6 %, respectively, higher than the USB's load.

Mortar with a lower w/c of 0.30 tends to form fewer capillary pores.

This is due to the higher density of the cement paste, which results in lower porosity and permeability because of reduced pore connectivity. As a result, it creates a denser and stronger cement matrix, particularly at the ITZ, where porosity is minimised. In contrast, a higher w/c of 0.50 can lead to excess water evaporating from the mixture, creating voids and weak zones within the mortar. Additionally, mortar with a low w/c ratio of 0.30 is likely to achieve complete cement hydration—benefiting from proper water curing and minimising unhydrated cement. This approach also reduces shrinkage due to lower water evaporation, promoting the formation of calcium silicate hydrate (CSH) gels, which enhance mechanical strength and reduce porosity. In Section 3.3, it is demonstrated that the mortar with a lower w/c of 0.30 exhibits significantly higher compressive, tensile, and flexural strength compared to mixes with a higher w/c of 0.50. The flexural strength of cement-based materials is largely determined by their tensile strength, which is directly affected by the w/c ratio. Denser concrete is more effective at resisting crack propagation and delaying failure under bending forces, resulting in higher flexural strength for RC beams. Indeed, carefully controlling the w/c ratio can ensure that RC beams achieve a higher flexural load capacity, better crack resistance, and longer service life due to enhanced durability, which helps minimise the ingress of harmful substances, thereby promoting sustainability. However, it is essential to handle low w/c mixtures carefully to maintain workability and ensure proper curing. The use of superplasticisers can assist in achieving this balance. Conversely, while a higher w/c ratio may improve workability, it compromises the strength and durability of the beams, ultimately leading to a reduced flexural load capacity.

This implies that RC beams should be strengthened with richer mortar than the normal strength mortar as the beams are damaged, which could occur due to any additional/unexpected loads such as earthquakes, wind loads, blasts, tsunamis, and fire. Interestingly, the damaged RC beams could reach their virgin (UCB) load-carrying capacity and even provide a higher load than the virgin beam, with 25 % and 50 % RCCB and a higher w/c of 0.50. Therefore, it is lighter, economical (low cost due to the low content of cement), and environment-friendly (since clinker production produces a significant amount of CO₂).

Figs. 5 and 6 show that replacement of NS beyond 50 % by RCCB decreases the flexural load of strengthened RC beams, which is consistent with the strength properties and porosity of the mortar fabricated with RCCB, as discussed in Section 3.3. The decrease in the average failure loads of the strengthened RC beams is about 6 % and 12 % for the w/c of 0.30 and 15 % and 25 % for the w/c of 0.50, respectively, lower than the USB. This could be linked to the higher porosity and lower mechanical strength of mortar fabricated with 75 % and 100 % RCCB. It is noted that the RCCB has a remarkable amount of coarser size particles and has descending strength properties and modulus of elasticity due to the higher porosity of RCCB than NS (Fig. 1), leading to lower strength properties and higher porosity of mortar [29]. Hence, it is recommended that up to 50 % RCCB be used as a replacement for NS to strengthen the RC beam.

The effect of the RCCB on enhancing the stiffness and deformed shape (sagging curvature) of strengthened beams is examined by comparing the deflections recorded at 3 points on the beams, as illustrated in Fig. 2. These measurements were obtained using LVDTs under a fixed flexural load of 100 kN, and the results are presented in Fig. 7. It is found that the incorporation of RCCB as a replacement of NS reduced the deflection of the strengthened RC beams and improved the stiffness as they were damaged. The deformed shapes of the USB and strengthened with 50 % RCCB are very close to each other, while the deformed shapes are more pronounced for strengthened with 75 % and 100 % RCCB mortar. The mid-point deflection of the USB and strengthened with 0 %, 25 %, and 50 % RCCB at 100 kN are $-0.61~\rm mm$, $-1.43~\rm mm$, $-1.13~\rm mm$ and $-0.84~\rm mm$, respectively, for a w/c of 0.30 and $-0.61~\rm mm$, $-1.68~\rm mm$, $-1.35~\rm mm$ and $-0.93~\rm mm$, accordingly, for a w/c of 0.50. The negative values represent the sagging curvature of the beams. This

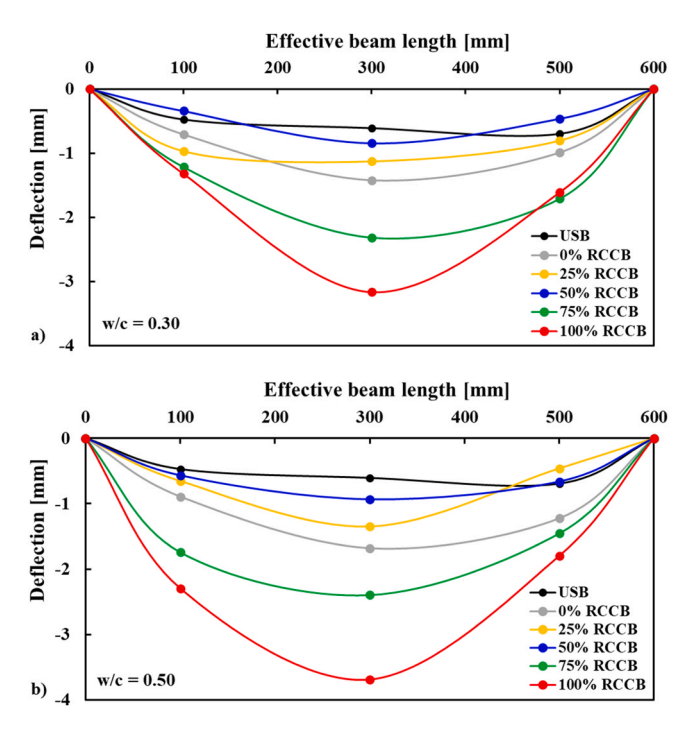


Fig. 7. Deformed shape at the load of 100 kN of USB and strengthened RC beams using ferrocement mortar made with different percentages of FCBP with w/c of 0.30 (a) and 0.50 (b).

implies that the strengthened RC beams with 25 % and 50 % RCCB are more effective in healing the cracks of the damaged beams and provide better load-deflection behaviour of the strengthened RC beams with 100 % NS and USBs.

Conversely, significantly more elevated deflection at beam failure was recorded in strengthened RC beams with up to 50 % RCCB than the USB and strengthened with 100 % NS. The average deflection of the beams at the failure of the USB and strengthened with 0 %, 25 %, and 50 % RCCB are 7.32 mm and 7.41 mm, 10.39 mm and 13.26 mm, respectively, for a w/c of 0.30 and 7.32 mm and 5.81 mm, 7.68 mm and 9.62 mm, accordingly, for a w/c of 0.50. This behaviour could be linked to the healing of the cracks, the better bond among parent concrete, ferrocement wire mesh, and RCCB mortar, thus enhancing the flexural load and providing more ductility of the beams (reinforcements inside the beams could allow yielding as the cracks and failure occur later). The increased ultimate deflection of strengthened beams fabricated with up to 50 % RCCB could support control of the early collapse of the structure. This enhancement provides occupants valuable time to escape during undeserved external loads, such as earthquakes, wind loads, and tsunamis.

3.2. Cracks patterns of RC beams

Fig. 8 shows the crack maps of USB and RC beams strengthened with ferrocement mortar at different percentages of RCCB, using w/c of 0.30 and 0.50. The inclined lines on the diagram represent the diagonal and flexural cracks in the RC beams, with their positions and lengths measured immediately after testing. As the flexural load in the beams grows, flexural cracks emerge around the mid-span of the RC beams and extend vertically to its height. Subsequently, diagonal cracks form as the flexural load continues to rise. Eventually, both diagonal and flexural cracks extend into the compression area of the RC beam, leading to collapse. There is a notable difference in crack patterns and quantities in the USBs and strengthened beams that use ferrocement with varying percentages of RCCB. The USBs exhibited fewer diagonal and flexural cracks (Fig. 8a, b) at the failure time. Conversely, the RC beams strengthened with 25 % and 50 % RCCB displayed a more significant

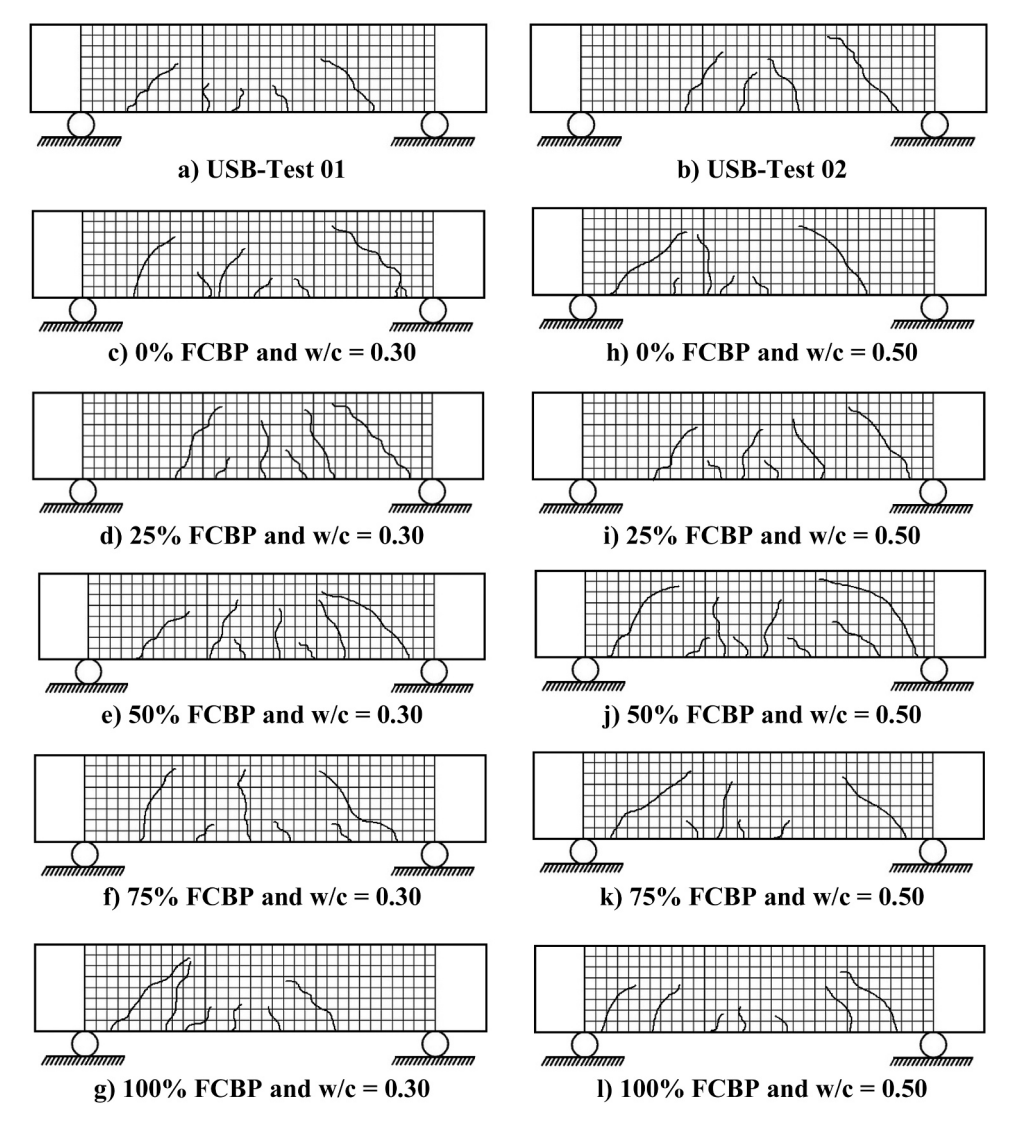


Fig. 8. Crack maps of USB (a-b), strengthened RC beams using ferrocement mortar with different percentages of FCBP and w/c of 0.30 (c-g) and 0.50 (h-l).

number of cracks along the entire length of the beam (Fig. 8e, j) when compared to the USB (Fig. 8a, b) and those strengthened with 0 % FCBP (Fig. 8c, h). This indicates that a ductile mode of failure occurred due to multiple cracks.

Enhancing the ductility of ferrocement-strengthened RC beams over USB can improve crack control and energy absorption due to steel wire mesh's high tensile strain capacity and its behaviour after cracking [16-20,25]. USBs may develop localised and wide cracks when subjected to certain flexural loads. However, the ferrocement's closely spaced steel wire mesh distributes these cracks into numerous fine microcracks. This behaviour delays the formation of critical cracks, thereby preventing sudden brittle failure. After initial cracking, the steel wire mesh bridges the cracks, maintaining load resistance even under high deformations. Additionally, the gradual yielding of the steel wire mesh and the longitudinal tension steel bars at the bottom of the beams may happen before cracks form at the interface between the steel wire mesh and the parent concrete surface, resulting in greater deflection [22, 25,26]. The pull-out resistance of the steel wire mesh also contributes to plastic deformation, enhancing the beam's deflection capacity. Furthermore, ferrocement serves as a ductile confinement layer as the steel wire meshes are wrapped around the damaged RC beam. This layer delays the buckling of compression steel and the crushing of concrete, which is especially beneficial in seismic zones where ductility is crucial [26].

It is noted that the RCCBs have a rough surface texture due to the production process induced by crushing bricks and being coarser than NS, which enriches the bond between RCCB mortar and the parent concrete and delays debonding at their interface. This observed failure behaviour aligns well with the author's previous study [22]. Additionally, no significant changes in crack patterns were noted for strengthened RC beams with w/c of 0.30 and 0.50.

Crack patterns, widths, and the number of cracks that occur under sustained loads and failure modes significantly impact the durability and longevity of RC beams. It has been found that ferrocement-strengthened RC beams exhibit thinner and more distributed cracks compared to USBs. This characteristic promotes a ductile failure mode by controlling crack formation and limiting crack width. The ductile flexural failure not only helps determine the residual strength of the beams but also enhances their repairability, which directly influences their service life. In contrast, the behaviour of ferrocement-strengthened RC beams significantly reduces the penetration of moisture and harmful chemicals when compared to USBs due to the better mechanical performance of ferrocement mortar (composed of a rich cement mixture, i.e., lower porosity and permeability). This reduction delays structural deterioration. The lower levels of corrosion ingress combined with ductile failure and smaller crack widths contribute to the overall longevity of the ferrocement-strengthened RC beams. As a result, ferrocementstrengthened RC beams demonstrate increased resistance to

environmental degradation, ultimately extending their service life and sustainability.

3.3. Mortar properties

3.3.1. Dry density of mortar mixes

The dry density of the ferrocement mortar fabricated with various replacement levels of NS by RCCB was recorded at 28 days on the same specimens used to perform compression tests and presented in Table 9. The density of mortar fabricated with RCCB is found to be significantly lower than that fabricated with 100 % NS. Compared to 100 % NS, the decrease in density of mortar fabricated with 50 % and 100 % RCCB are 14.74 % and 23.12 %, respectively, for the w/c of 0.30 and 15.15 % and 25.22 %, respectively, for the w/c of 0.50. This behaviour could be attributed to the descending unit weight (1120 kg/m³ for RCCB and 1594 kg/m³ for NS) and specific gravity (1.73 for RCCB and 2.22 for NS) of RCCB than NS. This lightweight RCCB mortar makes the strengthened beam lighter, reducing the structure's global dead load and reduced seismic forces. No remarkable change in the dry density was registered for the mortar fabricated with two different w/c of 0.30 and 0.50. Dang et al. [49] and Dang and Zhao [50] reported that concrete fabricated with waste clay bricks as fine aggregate has a lower density than concrete fabricated with NS. These outcomes are aligned with the present study.

3.3.2. Mechanical strength of mortar mixes

The 28-day compressive strength, tensile strength, and flexural strength of ferrocement mortar fabricated with different percentages of RCCB with two w/c are presented in Fig. 9. The dotted green and red lines represent the normalised strength. The strength of mortar was recorded to increase by up to 50 % in the replacement of NS by RCCB; beyond this replacement, the strength decreased. The enhancement in the mechanical strength of mortar fabricated with both w/c at 50 % RCCB is 17-22 % for compressive, 17-23 % for tensile, and 13-19 % for flexural strength compared to the mortar mix 100 % NS (0 % RCCB). This enhanced mechanical strength provides better load-bearing capacity for the strengthened RC beams than USBs.

The superior strengths of mortar fabricated with up to 50 % RCCB are due to the higher angular shape, excellent surface roughness, and coarser particles of RCCB than NS (Fig. 1), which enhances the bond between cement paste and RCCB, leading to higher strength. As shown in Fig. 1e, the scanning electron microscopy image of RCCB is higher angular and possesses a rougher surface than the NS. These advantageous properties offer superior mechanical properties to the mortar compared to mortar with NS. As reported in Table 2 and visual observation of Fig. 1b, the RCCB contains significantly higher amounts of finner particles, from 0.15 mm to pan, than NS. This higher amount of smaller-sized particles is anticipated to fill the micro and meso pores in the mortar matrix, improving the microstructure (lowering the porosity and pore connectivity, i.e., permeability) and densifying the interfacial transition zone (ITZ). This should enhance mechanical strength compared to 100 % normal sand (NS). In the following section, it is

Table 9Dry density of mortar mixes.

	Mix ID	Density [kg/m3]	Decrease [%]
W/C = 0.30	0 % FCBP	2398	0
	25 % FCBP	2179	9.12
	50 % FCBP	2044	14.74
	75 % FCBP	1976	17.60
	100 % FCBP	1843	23.12
W/C = 0.50	0 % FCBP	2349	0
	25 % FCBP	2113	10.06
	50 % FCBP	1993	15.15
	75 % FCBP	1920	18.29
	100 % FCBP	1757	25.22

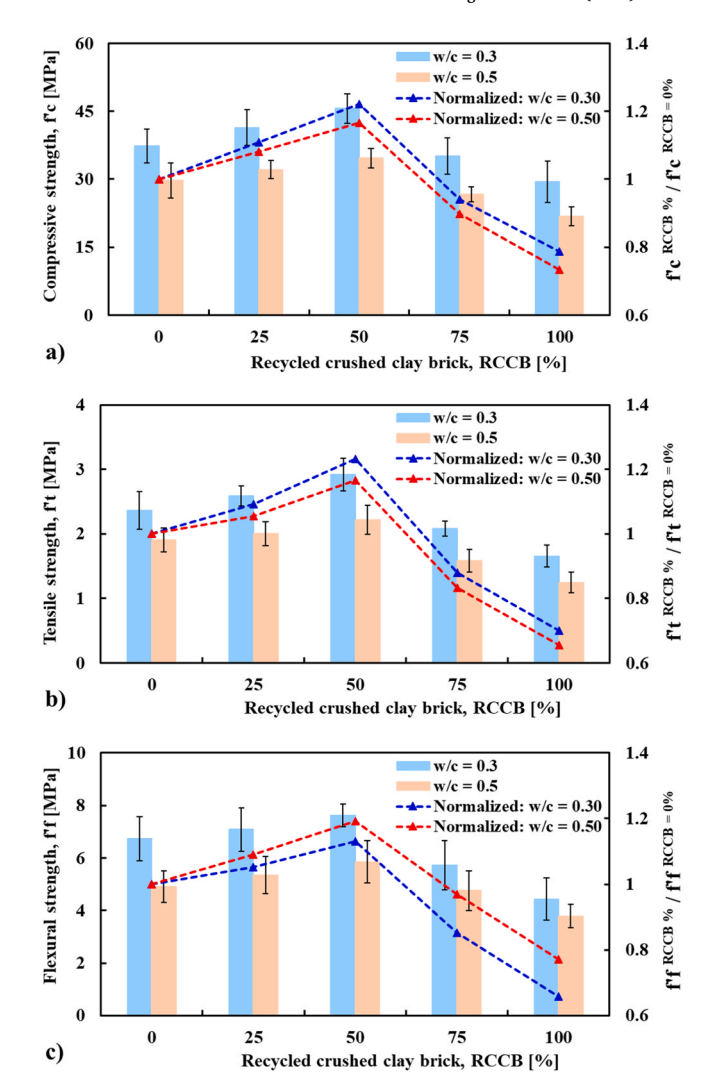


Fig. 9. Compressive strength- f_c (a), tensile strength- f_t (b), and flexural strength- f_f (c) of mortar mixes made with different replacement percentages of NS by FBCP and tested on the same day as the beam test.

reported that the porosity of mortar fabricated with up to 50 % RCCB decreased and increased beyond that level, which aligns with these two texts

In addition, the enhanced mechanical strength of RCCB mortar could be associated with the possible pozzolanic reaction due to RCCB's greater amount of finer particles, which are smaller than 0.15 mm to the pan, as shown in Table 2. The percentage passing of RCCB particle size 0.15 mm is approximately 2.1 times higher than the NS, and the amount of finner powder RCCB materials retained on the pan is about more than double that of the NS. These higher finner particles have a higher specific surface area for activating pozzolanic reactions in the mortar [51, 52]. This reaction could happen by reacting silica and alumina contents of RCCB with the cement hydrated products (Ca(OH)₂) and water in the mortar mix. This leads to constructing additional calcium silicate hydrate (C-S-H) gels, which augment the mechanical strength of the mortar mixes fabricated with RCCB [51,52].

The decrease in mechanical strength beyond 50 % replacement could be due to the higher porosity generated by a higher amount of coarser size particles (Table 2), lower Young's modulus and mechanical strength of RCCB than NS (RCCB contained more pores than NS, Fig. 1d, e). The declined strength could also be associated with the higher absorption capacity of RCCB compared to the NS (12.92 % for RCCB and 5.71 % for NS), which constructs defenceless ITZ by soaking water from its

neighbouring cement paste and increasing the unhydrated binder content in mortar mix, thus offer lower mechanical strength. The following section reveals that the porosity is increased for the mortar mixes fabricated with beyond 50 % RCCB, which is one of the key reasons for the decline in the strengths of the mixes. As expected, the higher mechanical strength of mortar with low w/c of 0.30 than w/c of 0.50 is due to the higher cement and lower water content in the mix.

3.3.3. Porosity of mortar mixes

Fig. 10 presents the 28-day porosity of mortar mixes fabricated with various substituent levels of RCCB with two different w/c. It has been observed that the porosity of ferrocement mortar is decreased up to 50 % replacement of NS by RCCB, and above this replacement, porosity increased. This result aligns with mortar's mechanical strength (Fig. 9). A maximum decline in porosity was observed at 50 % of RCCB, which is about 14 % for the w/c of 0.30 and 17 % for the w/c of 0.50. The lower porosity of the mortar mix with 50 % RCCB could be linked to reducing the micropores as a higher amount of finner-size particles smaller than 0.15 mm is observed (Table 2) in RCCB than in NS. This leads to filling the micropores of the mortar, offering lower porosity in the mortar mix. Furthermore, as reported earlier, the possible pozzolanic reaction of RCCB could produce secondary CSH gel [51,52], which fills the micro void and provides robust microstructure, leading to lower porosity, which is missing in the mortar fabricated with 100 % NS. Regarding beyond 50 % replacement, the increase in porosity could be linked to the higher amount of coarser size particles (Table 2) and higher porosity of RCCB (Fig. 1e), which could increase the void among the RCCB particles and increase the total porosity in the mix. This higher porosity of the mix with higher than 50 % RCCB aligns with the lower mechanical strength, as reported in Fig. 9. Miah et al. [29] also found that porosity decreased by 26 % when 50 % of waste clay bricks were used as a replacement for sand, which was due to a higher reduction of the micropores within the range of 74 μm to 150 μm , and below those sizes. Another study [30] revealed that the porosity decreased with the increased percentage of waste slag powder (42 % lower than the control mix with 100 % sand) due to significantly higher finer particle content (from 0.074 mm to 0.15 mm and even smaller, which significant reduction of the micropores within the range from 74 µm to 150 µm, and also for lower dimensions. Similar to mechanical strength, the higher porosity of mixes with higher w/c of 0.50 than lower w/c of 0.30, which is associated with the lower amount of binder and higher amount of water in the mix.

Fig. 11 illustrates the correlation between strengths (compressive, flexural, and tensile) and porosity, with the results compared to existing models in the literature [53–57]. It is clearly observed that as the compressive, flexural, and tensile strength decreased, the porosity increased. The relationship is quite linear and aligns well with existing literature [53–57]. This study proposes Eqs. (4–9) to calculate the porosity of ferrocement mortar once its strength is known or vice versa. For $\rm w/c=0.30$

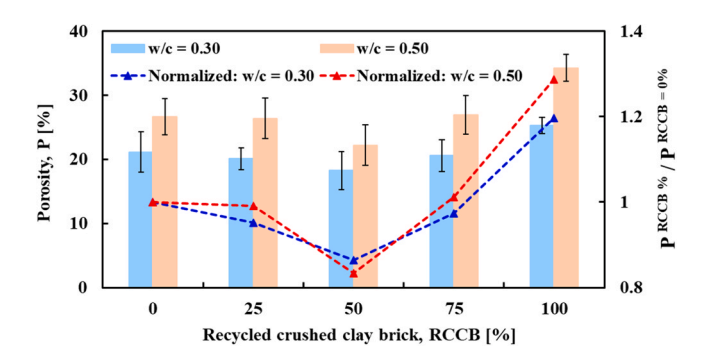


Fig. 10. The porosity of mortar mixes made with different replacement percentages of NS by FCBP with a water-to-cement of 0.30 and 0.50.

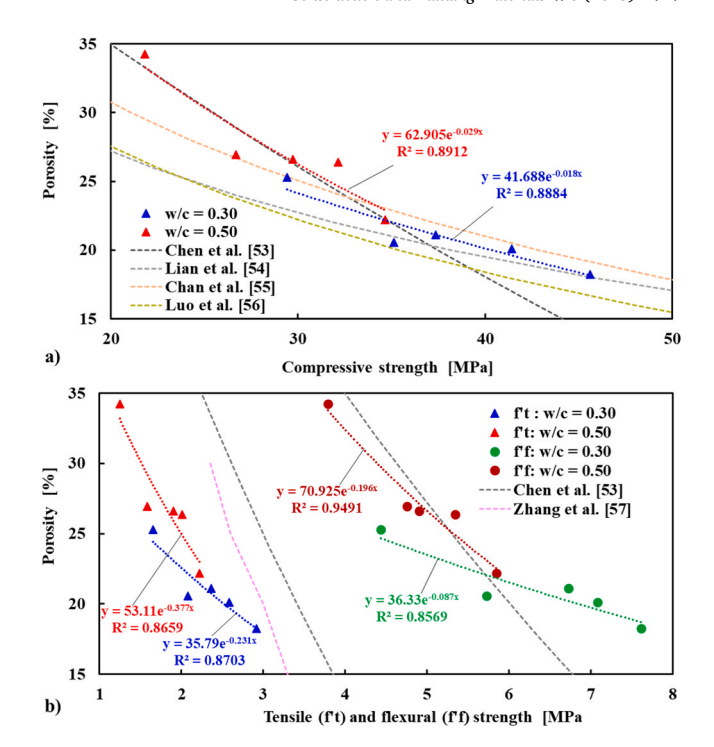


Fig. 11. Correlation of porosity (P) with compressive strength- f_c (a), tensile strength- f_t and flexural strength- f_f (b), and justified with models found in the literature [53–57].

$$P = 41.688e^{-0.018 * f_c}R^2 = 0.88(28 - \text{day compressive strength})$$
 (4)

$$P = 35.79e^{-0.231 * f_t}$$
 $R^2 = 0.87(28 - \text{day tensile strength})$ (5)

$$P = 36.33e^{-0.087 * f_f}R^2 = 0.85(28 - \text{day flexural strength})$$
 (6)

For w/c = 0.50

$$P = 62.905e^{-0.029 * f_c}R^2 = 0.89(28 - \text{day compressive strength})$$
 (7)

$$P = 53.11e^{-0.377 * f_t}$$
 $R^2 = 0.86(28 - \text{day tensile strength})$ (8)

$$P = 70.925e^{-0.196 * f_f} R^2 = 0.94(28 - \text{day flexural strength})$$
 (9)

where f_c is compressive strength, f_t is splitting tensile strength, f_f is the flexural strength and P is porosity.

As reported in Figs. 9 and 10, ferrocement-strengthened RC beams' significantly higher mechanical strength and lower porosity can provide long-term durability. Reduced porosity results in fewer voids within the material, leading to decreased permeability due to lower pore connectivity (though it needs to be confirmed by further tests), a more robust microstructure, and improved mechanical properties [58]. Fig. 11 illustrates that as porosity decreases, the mortar's compressive, tensile, and flexural strength increases, which aligns with findings in the literature [53–58]. This lower porosity not only enhances the mechanical strength of the mortar but also improves the beams' ability to withstand heavy loads, as reported in Figs. 5 and 6. This denser microstructure of RCCB mortar could limit the penetration of harmful water, chlorides, sulfates, and other corrosive agents to the RC beams, thereby preventing corrosion of the steel reinforcement and the ferrocement steel wire mesh. Additionally, lower porosity contributes to reduced creep and shrinkage [29,30] in mortar or concrete by minimising water evaporation and microcrack formation. It also strengthens the adhesion to reinforcement, reduces slippage, and enhances composite action in the RC beams. Miah et al. [58] studied the long-term strength and durability performance of concrete with supplementary cementitious materials for up to 900 days. The results show that the pozzolanic action and filler effect significantly improve mechanical strength, create robust microstructures, enhance the interfacial transition zone (ITZ) between cement paste and aggregates (assessed at 730 days), and lower porosity and water absorption capacity tested in all ages up to 900 days, which collectively demonstrate enhanced long-term durability of the concrete [58]. Overall, the reduced porosity (indicating lower permeability due to decreased pore connectivity) of the RCCB mortar can enhance the load capacity, longevity, and resilience of ferrocement-strengthened RC beams. This improvement ensures RC beams' overall stability and safety while reducing the need for frequent repairs and maintenance. To verify these properties and before drawing any firm conclusion for applying them in the actual application, further investigations are necessary into the durability and long-term performance of the RCCB mortar and ferrocement-strengthened beams exposed to different aggressive weathering actions.

4. Data-based model results

In the first step, a representative model for each case based on their different percentages of RCCB with w/c of 0.30 and 0.50 have been developed. Later, the developed model has been validated with a different set of test data. The data-based model and validation of the load versus mid-point deflection profiles are depicted in Fig. 12. To make a realistic scenario, three cases (e.g., 0 %, 50 %, and 100 % RCCB) have been selected for data modelling and validation for both w/c of 0.30 and 0.50. In a nutshell, the modell's performances of those selected cases, i.e., 0 %, 50 %, and 100 % RCCB, are pretty good. Additionally, it is observed that for almost all of the aforementioned cases, the validation results confirm the developed model's efficacies.

Similar to the load-deflections trajectories, the model development

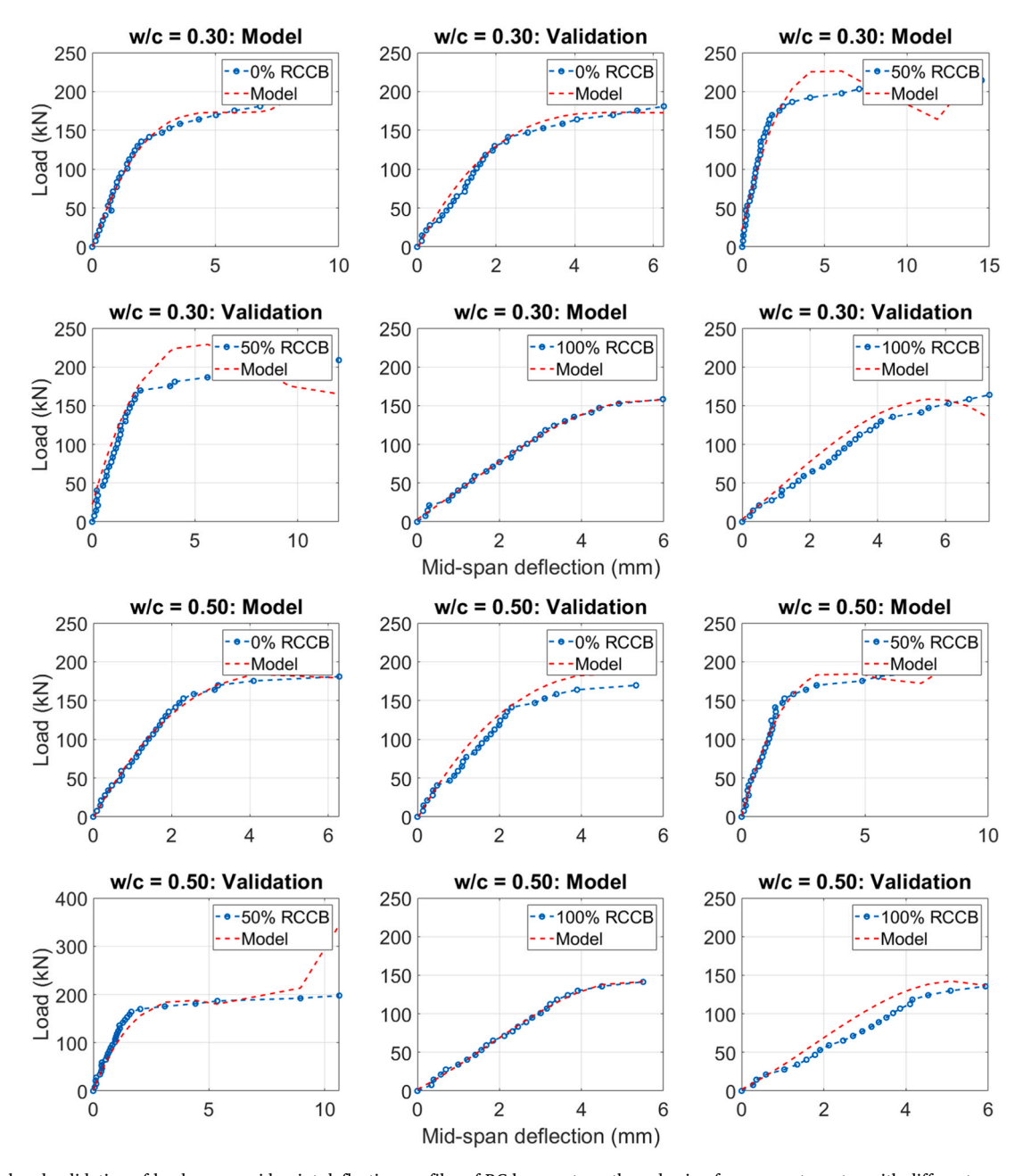


Fig. 12. Model and validation of load versus mid-point deflection profiles of RC beams strengthened using ferrocement mortar with different percentages of RCCB with w/c of 0.30 and 0.50.

and verification of compressive strength, flexural strength, and tensile strength for both w/c of 0.30 and 0.50 have been performed. In this case, for strengths cases, three different data sets are used to develop the model, while the validation is performed by using their average value. Fig. 13 shows the compressive strength, flexural strength, and tensile strength outcomes for both w/c of 0.30 and 0.50. Herein, the pretty good accuracy of the model can be noticed both in the model performance comparison and validation.

Furthermore, the model has been developed, and the model's performances have been validated for the porosity at both w/c of 0.30 and 0.50 in Fig. 14. In this case, the model performance comparison and the validation results are also observed to confirm the developed models' efficacy. Despite the excellent performances of those models, all aforesaid models can be made more accurate by changing their model orders, but that would lead to overfitting and over parameterised models, which has been avoided here. However, all the developed models will be updated by utilising more experimental data. Further, it is also planned to optimise the performances of the existing models via nonlinear optimisation algorithms. After analysing all of the above results, it can be summarised that in all cases, the results from the w/c of 0.5 is more coherent than the w/c of 0.3. In contrast, the beams with 100 % RCCB seem smoother than their counterpart with 50 % RCCB 50. All of the developed models can be utilised to give an idea of the expected outcome for future studies without making any real beams. Based on the model's outcome, designers can decide what kind of specimen/beam will be built for a more detailed study.

In the final step, two load-deflection curves of ferrocementstrengthened RC beams from Megarsa and Kenea [59] have been extracted and compared with the data-based model to validate the efficiency of the proposed model, as shown in Fig. 15.

It has been found that the proposed data-based model mirrored the experimental load-deflection curves from Megarsa and Kenea [59] accurately, which demonstrated the excellent performance of the proposed model, which could be used to analyse the ferrocement-strengthened RC beams. However, this model is currently in the development stage, where authors are working on tuning and optimising model performances.

5. Conclusions

This study examines the impact of recycled crushed clay brick (RCCB) on the flexural performances of strengthened RC beams using ferrocement mortar with various substitute levels (0, 25, 50, 75 and 100 %) of natural sand (NS) by RCCB with two different w/c of 0.30 and 0.50. The RCCBs are produced in large quantities while breaking the old waste clay bricks to make coarse aggregate, which was sieved and used to replace NS. To understand the impact of RCCB on the flexural behaviour of strengthened RC beams, the mechanical strength and porosity of the ferrocement mortar were investigated. The main findings of this study are presented below.

- I. The strengthened RC beams using ferrocement mortar fabricated with 100 % NS (0 % RCCB) exhibited higher flexural load than un-strengthened beams (USBs). It should be noted that two USBs were loaded until they collapsed.
- II. The incorporation of RCCB up to 50 % replacement of NS enhances the flexural load-carrying capacity of RC beams, which is about 15 % higher than that of the USB. This could be associated with the higher tensile strength of steel wire mesh, better confining effect, limiting crack formation and propagation and a stronger bond among the parent concrete (roughening old concrete surfaces by chipping), steel wire mesh, and RCCB mortar. Also, the 50 % RCCB mix has better mechanical strength and lower porosity than the 100 % NS mix.
- III. The damaged beams strengthened with 50 % RCCB were able to nearly reach the stiffness of the virgin beam and provide higher

- deflection (81 % for a w/c of 0.30 and 31 % for a w/c of 0.50 higher than 100 % USB) with ductile failure induced by multiple flexural and diagonal cracks. This behaviour is related to the closely spaced steel wire mesh in ferrocement, which distributes cracks into numerous fine microcracks. This helps delay critical cracks and results in a ductile failure mode.
- IV. The increase in RCCB content beyond the 50 % replacement level leads to a decreased flexural load of strengthened beams. This behaviour agrees with the higher porosity and lower strengths of mortar beyond the 50 % replacement of NS by RCCB.
- V. The RCCBs are highly angular in shape, coarser particles, and have excellent surface roughness, and also contain a higher amount of finner size particles smaller than 0.15 mm than NS (2.1 times higher than the NS). Hence, this higher content of RCCB finer powder is expected to fill the microvoids (lowering the porosity and reducing the pore connectivity, i.e., reducing permeability, healing the cracks, and densifying the ITZ). This leads to augmenting the strength properties and reducing the mortar's porosity with 50 % RCCB rather than 100 % NS.
- VI. The proposed data-based modelling exhibited excellent outcomes and correctly predicted the experimental results, including loaddeflection of the beans, mechanical strength (compressive, flexural, and tensile), and porosity of the mortar mixes. This simple data modelling could be a powerful alternative to physical experiments, which are economical, less time-consuming, and less involved in the workforce.

Overall, strengthening using ferrocement mortar with 50 % RCCB is lighter (15 % lower density than NS, which reduces the dead load of the structures and seismic force) and more ductile due to higher deflection and multiple cracks. These properties help to prevent premature collapse and give occupants more time to escape during severe events or undesirable loads like earthquakes or intense wind loads. The use of RCCB is economical since it is made from waste products of brick aggregate. This approach conserves significant amounts of natural resources, addresses waste disposal issues, contributes to sustainable development, and helps protect the environment. The ferrocement technique is a more straightforward construction process and has better ductility than other techniques that utilise locally available materials, which helps save construction time. For instance, Joyklad et al. [19] investigated the 9 slabs that were strengthened with ferrocement jackets, 3 with carbon fibre reinforced polymer (CFRP), and 2 with glass fibre reinforced polymer (GFRP) jackets, where 3 sizes of welded wire mesh were used (small, medium, and large). The authors [19] stated that applying the ferrocement wire mesh with mechanical anchors did not significantly enhance the peak loads (i.e., the maximum enhancement was limited to 14.29 %) compared to the strengthened by CFRP and GFRP. However, a significant improvement in the ductility was observed for the strengthened slab with ferrocement wire mesh compared to CFRP and GFRP, which is approximately 94.14 %-119.07 % higher than the control one [19]. Similarly, Ganesan et al. [60] investigated the flexural strengthening of RC beams using FRPs and ferrocement. They [60] found that the ferrocement showed a better performance in terms of ductility than CFRP and GFRP. Živkovic et al. [61] stated that ferrocement is a versatile solution for strengthening structures, offering superior ductility, improved shear strength, and greater moment capacity than FRP sheets. It also has better fire and corrosion resistance than steel [61]. Both cast-in-place and precast ferrocement composites are cost-effective and don't require specialised materials or highly trained labour [61]. Therefore, it is suggested to utilise up to 50 % RCCB as a substitute for NS for strengthening the RC beam and with rich mortar (with low w/c of 0.30) to limit the penetration of water (i.e., lower permeability, lower risk of corrosion), given the reduced net cover and increased surface area of the reinforcement. This RCCB ferrocement strengthening technique can be applied to several reinforced concrete structural elements without compromising mechanical performance,

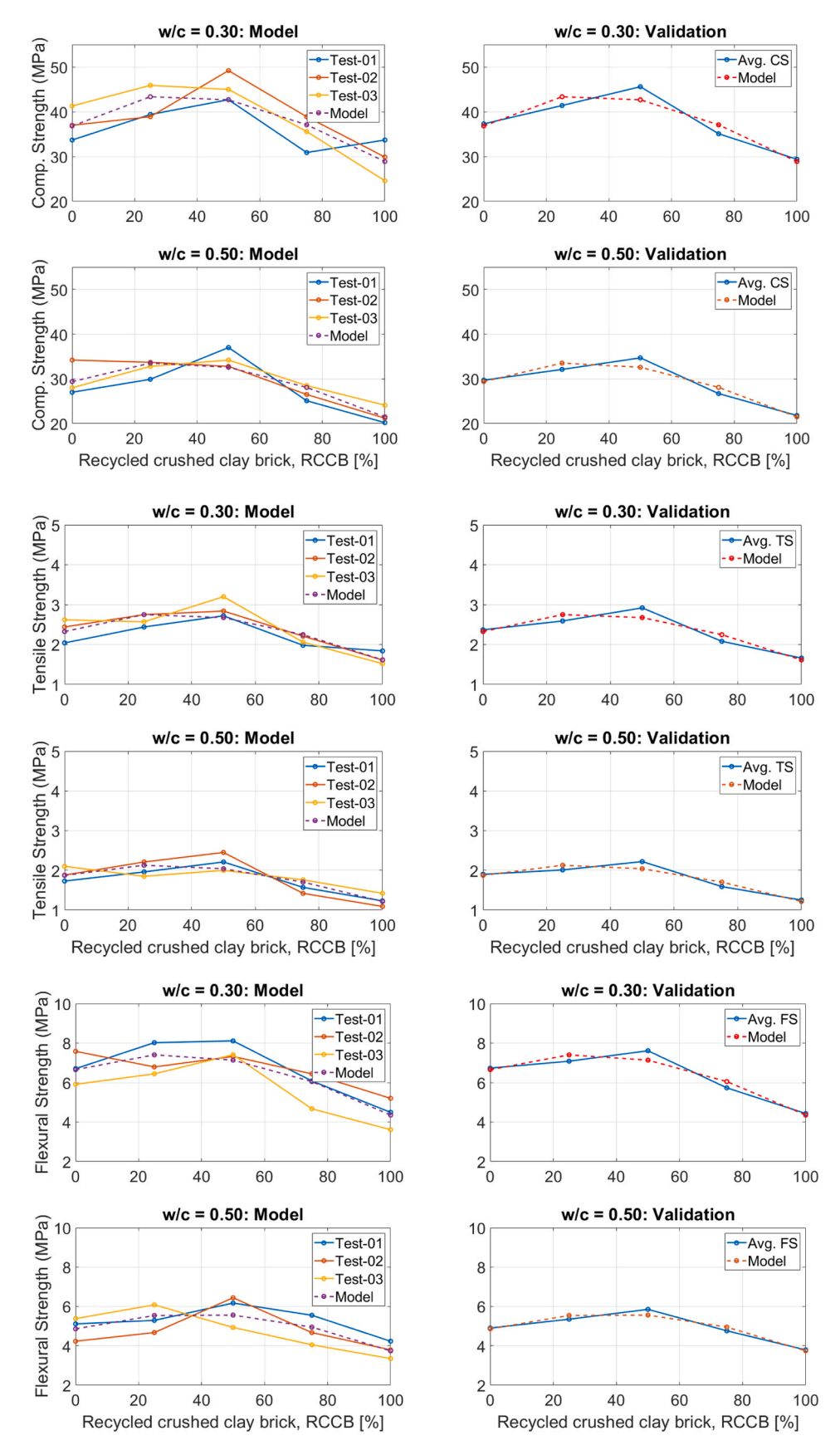


Fig. 13. Model and validation of compressive strength (CS), tensile strength(TS), and flexural strength (FS) of mortar mixes fabricated with various substituent levels of NS by RCCB tested on the same day of the beam test.

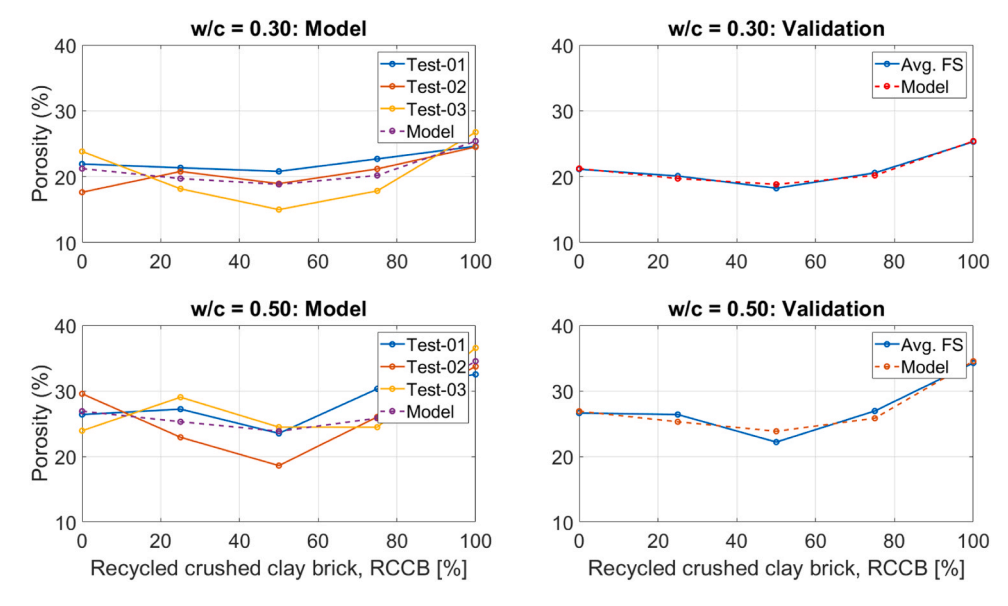


Fig. 14. Model and validation for the porosity of mortar mixes fabricated with various substituent levels of NS by RCCB with w/c of 0.30 and 0.50.

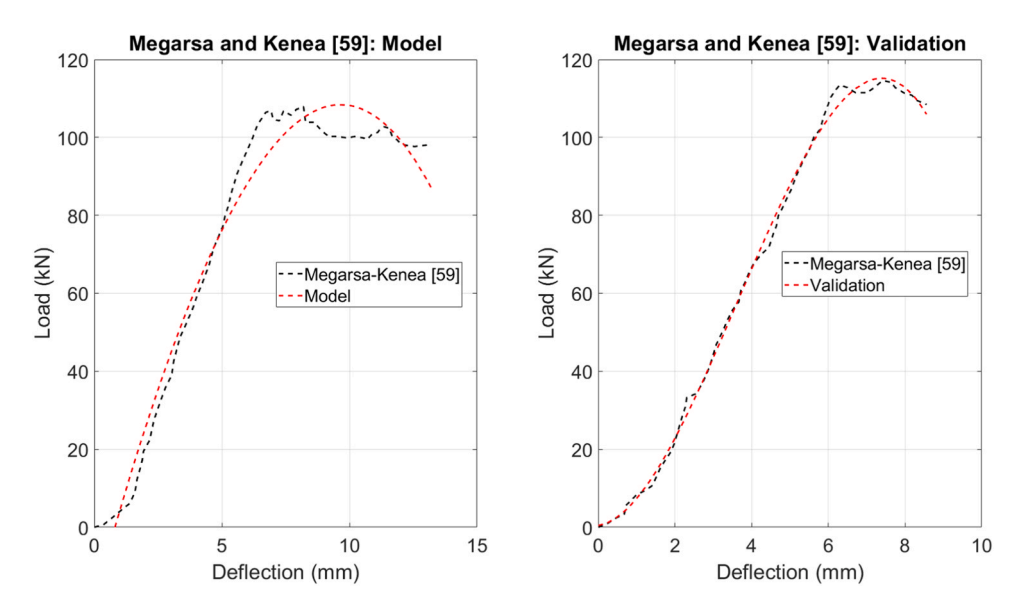


Fig. 15. Comparison of the experimental load-deflection curves of two RC beams strengthened using ferrocement from the literature (Megarsa and Kenea [59]) with the proposed data-based model.

which promotes sustainability.

The present research on ferrocement strengthening with RCCB mortar opens up numerous exciting opportunities for future studies, including its application in various structural elements such as columns, walls, and slabs under different load conditions. Future investigations could focus on the long-term durability of these structures in harsh environments through accelerated ageing tests, fire resistance assessments [6,62], and sustainability evaluations of ferrocement-reinforced structures. Additionally, optimising design through computational modelling and AI-driven analysis, incorporating fibres to enhance the ductility of ferrocement mortar, and using multi-layer steel wire mesh configurations could further improve performance. Research into cost-effective construction techniques and large-scale implementations in seismic or extreme environments would also be beneficial, along with integrating innovative technologies for real-time structural health monitoring. Advancements in computational modelling and non-destructive testing methods could refine design guidelines, and optimising the performance of data-based modelling through nonlinear optimisation algorithms is necessary to reflect the experimental results more accurately. These further studies could make ferrocement a more widely adopted solution in modern construction.

CRediT authorship contribution statement

Miah Md Jihad: Writing – review & editing, Writing – original draft, Visualization, Validation, Supervision, Resources, Project administration, Methodology, Investigation, Funding acquisition, Formal analysis, Data curation, Conceptualization. Li Ye: Writing – review & editing. Hasan Noor Md. Sadiqul: Writing – review & editing. Miah Mohammad Shamim: Writing – review & editing, Writing – original draft, Software, Investigation, Formal analysis, Data curation. Sobuz Md. Habibur Rahman: Writing – review & editing.

Declaration of Competing Interest

The authors declare no conflict of interest.

Acknowledgements

The authors acknowledge facilities provided by the Department of Civil Engineering, University of Asia Pacific (UAP), to undertake this research. Thanks to S.U. Sagar, M.R. Islam, and M. Akter for participating in this research project during their undergraduate thesis. A special thanks to Md. Kawsar Ali and Md. Monirul Islam, for performing part of the tests.

Data Availability

Data will be made available on request.

References

- A. Abdelrahman, Strengthening of Concrete Structures-Unified Design Approach, Numerical Examples and Case Studies, Springer Nature Singapore Pte Ltd, 2023, https://doi.org/10.1007/978-981-19-8076-3.
- [2] M. Engindeniz, L.F. Kahn, A.-H. Zureick, Repair and Strengthening of Reinforced Concrete Beam-Column Joints: State of the Art, 102 (2005) 1-14.
- [3] Y. Zhua, Y. Zhang, H.H. Husseinc, G. Chen, Flexural strengthening of reinforced concrete beams or slabs using ultrahigh performance concrete (UHPC): a state of the art review, Eng. Struct. 205 (2020) 110035.
- [4] A. Siddika, M.A.Al Mamun, R. Alyousef, Y.H.M. Amran, Strengthening of reinforced concrete beams by using fiber-reinforced polymer composites: a review, J. Build. Eng. 25 (2019) 100798.
- [5] M.S. Miah, M.J. Miah, M.M. Hossain, S.C. PaulNonlinear seismic response of flat plate systems made with ultra low strength concrete, Global Science and Technology Journal/2028, 6 (2) pp. 35-46(https://zantworldpress.com/product /june-2018-global-science-technology-journal/).
- [6] M.J. Miah, P. Pimienta, H. Carré, N. Pinoteau, C.La Borderie, Fire spalling of concrete: Effect of cement type, Proceedings of the 4th RILEM International Workshop on Concrete Spalling due to Fire Exposure, Leipzig, Germany, 2015.
- [7] M.J. Miah, F. Lo Monte, R. Felicetti, P. Pimienta, H. Carré, C.La Borderie, Impact of external biaxial compressive loading on the fire spalling behavior of normalstrength concrete, Constr. Build. Mater. 366 (2023) 130264.
- [8] J. Liu, X. Fan, L. Zou, C. Shi, Effect of different CFRP strengthening methods on fracture parameters of concrete beam, Eng. Fract. Mech. 314 (2025) 110748.
- [9] Y. Zhang, F. Zhang, L. Wu, H.-Z. Han, Y.-F. Wu, Flexural capacity design model of reinforced concrete beams strengthened with hybrid bonded CFRP, Eng. Struct. 319 (2024) 118822.
- [10] E. Fathalla, B. Mihaylov, Shear behaviour of deep beams strengthened with highstrength fiber reinforced concrete jackets, Eng. Struct. 325 (2025) 119404.
- [11] S. Etienot, H. Xargay, M. Ripani, A. Caggiano, P. Folino, Strengthening of existing reinforced concrete beams by self compacting fiber reinforced concrete jackets, Constr. Build. Mater. 448 (2024) 138233.
- [12] T. Liu, H. Wang, D. Zou, X. Long, M.J. Miah, Y. Li, Strength recovery of thermally damaged high-performance concrete subjected to post-fire carbonation curing, Cem. Concr. Compos. 143 (2023) 105273.
- [13] M.J. Miah, J. Thygesen, M.E. Simonsen, R.P. Nielsen, M. Wu, Strengthening the bulk properties of cement mortar through promoted in-situ formation of hydroxyapatite: Feasibility and perspectives, Constr. Build. Mater. 459 (2025) 139773.
- [14] J. Zhou, J. Leng, J. Yang, Z. Zhang, J. Du, Y. Zou, Experimental investigation on shear behavior of damaged and acid rain-corroded RC T-beams strengthened with ultra-high-performance concrete, Eng. Struct. 327 (2025) 119618.
- [15] H. Feng, S. Wang, W. Wang, Z. Yang, J. Zhu, K. Li, Flexural behaviour of reinforced concrete beams strengthened with ultra-high ductility MPC-based composites, Structures 71 (2025) 108052.
- [16] A. Mukherjee, H.B. Kaushik, Strengthening of unreinforced masonry buildings with ferrocement composite overlay: material characterisation and numerical study, Case Stud. Constr. Mater. 22 (2025) e04177.
- [17] Irfanullah, A. Gul, K. Khan, I.U. Khan, H.M.S. ElDin, M. Azab, K. Shahzada, Improving the lateral load resistance capacity of cellular lightweight concrete (CLC) block masonry walls through ferrocement overlay, Appl. Eng. Sci. 18 (2024) 100180
- [18] A.M. Abdallah, M. Badawi, G. Elsamak, J.W. Hu, E.A. Mlybari, M. Ghalla, Strengthening of RC beams with inadequate lap splice length using cast-in-situ and anchored precast ECC ferrocement layers mitigating construction failure risk, Case Stud. Constr. Mater. 20 (2024) e02747.
- [19] P. Joyklad, C.K. Gadagamma, B. Maneengamlert, A. Nawaz, A. Ejaz, Q. Hussain, P. Saingam, Structural behavior of RC one-way slabs strengthened with ferrocement and FRP composites, Eng. Fail. Anal. 161 (2024) 108328.
- [20] M.E. Elnagar, M.H. Makhlouf, K.M. El-Sayed, G.I. Khaleel, An experimental and numerical study on two-way RC slabs with openings strengthened by ferrocement technique. Structures 65 (2024) 106673.
- [21] C.-K. Ma, N.M. Apandi, S.C.S. Yung, N.J. Hau, L.W. Haur, A.Z. Awang, W. Omar, Repair and rehabilitation of concrete structures using confinement: A review, Constr. Build. Mater. 133 (2017) 502–515.
- [22] M.J. Miah, M.S. Miah, W.B. Alam, F. Lo Monte, L. Ye, Strengthening of RC beams by ferrocement made with unconventional concrete, Mag. Civ. Eng. 89 (5) (2019) 94–105.

- [23] ACI Committee 549 (ACI549-88R), State-of-the-Art Report on Ferrocement. American Concrete Institute, Detroit, 1988, pp 24.
- [24] ACI Committee 549 (ACI549.1-88R), Guide for the Design, Construction, and Repair of Ferrocement. American Concrete Institute, Detroit, 1988, pp.27.
- [25] P. Paramasivam, C.T.E. Lim, K.C.G. Ong, Strengthening of RC beams with ferrocement laminates, Cem. Concr. Compos. 20 (1998) 53–65.
- [26] M.S. Miah, M.J. Miah, M.M. Hossain, S.C. Paul, Seismic retrofit of flat plate and flat slabs using ferrocement. Proc. of the 5th ICONTES, p. 12, Kuala Lumpur, Malaysia, February 01-02, 2018.
- [27] P. Domone, J. Illston. Construction Materials: Their Nature and Behaviour, 4Fourth ed., Spon Press, 270 Madison Avenue: New York, NY, USA, 2010.
- [28] M.J. Miah, R. Huaping, S.C. Paul, A.J. Babafemi, R. Sharma, J.G. Jang, Performance of eco-friendly concrete made from recycled waste tire fine aggregate as a replacement for river sand, Structures 58 (2023) 105463.
- [29] M.J. Miah, S.U. Sagar, S.C. Paul, A.J. Babafemi, Feasibility of using recycled burnt clay brick waste in cement-based mortar: Mechanical properties, durability, and residual strength after exposure to elevated temperatures, Int. J. Civ. Eng. 19 (2021) 1055–1069.
- [30] M.J. Miah, M.K. Ali, F. Lo Monte, S.C. Paul, A.J. Babafemi, B. Šavija, The effect of furnace steel slag powder on the performance of cementitious mortar at ambient temperature and after exposure to elevated temperatures, Structures 33 (2021) 2811–2823.
- [31] Q. Huang, X. Zhu, G. Xiong, C. Wang, D. Liu, L. Zhao, Recycling of crushed waste clay brick as aggregates in cement mortars: An approach from macroscale investigation, Constr. Build. Mater. 274 (2021) 122068.
- [32] ASTM C127-15, Standard Test Method for Relative Density (Specific Gravity) and Absorption of Coarse Aggregate, ASTM International, West Conshohocken, PA, USA, 2015.
- [33] ASTM C128-15, Standard Test Method for Relative Density (Specific Gravity) and Absorption of Fine Aggregate, ASTM International, West Conshohocken, PA, USA, 2015
- [34] ASTM C29/C29M-17a, Standard Test Method for Bulk Density ("Unit Weight") and Voids in Aggregate, ASTM International, West Conshohocken, PA, USA, 2017.
- [35] ASTM C136/C136M-14, Standard Test Method for Sieve Analysis of Fine and Coarse Aggregates, ASTM International, West Conshohocken, PA, USA, 2014.
- [36] ASTM Cl31 / Cl31M-14, Standard Test Method for Resistance to Degradation of Small-Size Coarse Aggregate by Abrasion and Impact in the Los Angeles Machine, ASTM International, West Conshohocken, PA, USA, 2006.
- [37] BS EN 1097-3:1998, Tests for mechanical and physical properties of aggregates-Determination of loose bulk density and voids, British Standard Institutions, London, UK, 1998.
- [38] ASTM C187-16, Standard Test Method for Amount of Water Required for Normal Consistency of Hydraulic Cement Paste, ASTM International, West Conshohocken, PA, USA, 2016.
- [39] ASTM C191-19, Standard Test Methods for Time of Setting of Hydraulic Cement by Vicat Needle, ASTM International, West Conshohocken, PA, USA, 2019.
- [40] ASTM C109/C109M-16a, Standard Test Method for Compressive Strength of Hydraulic Cement Mortars (Using 2-in. or [50-mm] Cube Specimens), ASTM International, West Conshohocken, PA. USA, 2016.
- [41] ASTM C307-18, Standard Test Method for Tensile Strength of Chemical-Resistant Mortar, Grouts, and Monolithic Surfacings, ASTM International, West Conshohocken, PA, USA, 2018.
- [42] ASTM C143/C143M-20, Standard Test Method for Slump of Hydraulic-Cement Concrete, ASTM International, West Conshohocken, PA, 2020.
- [43] ASTM C39/C39M-18, Standard Test Method for Compressive Strength of Cylindrical Concrete Specimens, ASTM International, West Conshohocken, PA, USA, 2018.
- [44] ASTM C496/C496M-17, Standard Test Method for Splitting Tensile Strength of Cylindrical Concrete Specimens, ASTM International, West Conshohocken, PA, USA, 2017.
- [45] NF P18-459, Essai Pour Béton durci-Essai De Porosité et De Masse Volumique, AFNOR, La Plaine, France, 2010.
- [46] ASTM C348-19, Standard Test Method for Flexural Strength of Hydraulic-Cement Mortars, ASTM International, West Conshohocken, PA, USA, 2019.
- [47] S.M. Stephen, Gergonne's 1815 paper on the design and analysis of polynomial regression experiments, Hist. Math. 1 (4) (1974) 431–439, https://doi.org/ 10.1016/0315-0860(74)90033-0.
- [48] J. Fan, Local Polynomial Modelling and Its Applications: From linear regression to nonlinear regression. Monographs on Statistics and Applied Probability, Chapman & Hall/CRC, 1996. ISBN 978-0-412-98321-4.
- [49] J. Dang, J. Zhao, W. Hua, Z. Du, D. Gao, Properties of mortar with waste clay bricks as fine aggregate, Constr. Build. Mater. 166 (2018) 898–907.
- [50] J. Dang, J. Zhao, Influence of waste clay bricks as fine aggregate on the mechanical and microstructural properties of concrete, Constr. Build. Mater. 228 (2019) 116757.
- [51] T. Vieira, A. Alves, J. de Brito, J.R. Correia, R.V. Silva, Durability-related performance of concrete containing fine recycled aggregates from crushed bricks and sanitary ware, Mater. Des. 90 (2016) 767–776.
- [52] J.M. Khatib, Properties of concrete incorporating fine recycled aggregate, Cem. Concr. Res. 35 (2005) 763–769.
- [53] X. Chen, S. Wu, J. Zhou, Influence of porosity on compressive and tensile strength of cement mortar, Constr. Build. Mater. 40 (2013) 869–874.
- [54] C. Lian, Y. Zhuge, S. Beecham, The relationship between porosity and strength for porous concrete, Constr. Build. Mater. 25 (2011) 4294–4298.

- [55] Y.N. Chan, X. Luo, W. Sun, Compressive strength and pore structure of highperformance concrete after exposure to high temperature up to 800 oC, Cem. Concr. Res. 30 (2000) 247–251.
- [56] X. Luo, W. Sun, S.Y.N. Chan, Effect of heating and cooling regimes on residual strength and microstructure of normal strength and high-performance concrete, Cem. Concr. Res. 30 (2000) 379–383.
- [57] S. Zhang, K. Cao, C. Wang, X. Wang, G. Deng, P. Wei, Influence of the porosity and pore size on the compressive and splitting strengths of cellular concrete with millimeter-size pores, Constr. Build. Mater. 235 (2020) 117508.
- [58] M.J. Miah, R. Huaping, S.C. Paul, A.J. Babafemi, Y. Li, Long-term strength and durability performance of eco-friendly concrete with supplementary cementitious materials, Innov. Infrastruct. Solut. 8 (2023) 255.
- [59] E. Megarsa, G. Kenea, Numerical Investigation on Shear Performance of Reinforced Concrete Beam by Using Ferrocement Composite, Math. Probl. Eng. (2022). Article ID 5984177, 12.
- [60] N. Ganesan, P. Bindurania, P.V. Indira, Flexural strengthening of RCC beams using FRPs and ferrocement - a comparative study, Adv. Concr. Constr. 10 (2020) 35–48.
- [61] D. Živkovic, P. Blagojevic, D. Kukaras, R. Cvetkovic, S. Rankovic, Comprehensive Analysis of Ferrocement-Strengthened Reinforced Concrete Beam, Buildings 14 (2024) 1082.
- [62] M.J. Miah, The Effect of Compressive Loading and Cement Type on the Fire Spalling Behaviour of Concrete (Ph.D. Thesis), Université de Pau et des Pays de l'Adour, Pau, France, October 2017.